IEEE Access
Multidisciplinary | Rapid Review | Open Access Journal

Received September 10, 2018, accepted October 7, 2018, date of publication October 18, 2018, date of current version April 5, 2019.

Digital Object Identifier 10.1109/ACCESS.2018.2876646

OFDM Signal Recovery in Deep Faded Erasure Channel

ALIREZA RAHMATI[1], KAAMRAN RAAHEMIFAR[1], (Senior Member, IEEE), THEODOROS A. TSIFTSIS[2], (Senior Member, IEEE), ALAGAN ANPALAGAN[1], (Senior Member, IEEE), AND PAEIZ AZMI[3], (Senior Member, IEEE)

[1]Department of Electrical and Computer Engineering, Ryerson University, Toronto, ON M5B 2K3, Canada
[2]School of Electrical and Information Engineering, Jinan University, Zhuhai 519070, China
[3]Department of Electrical and Computer Engineering, Tarbiat Modares University, Tehran, Iran

Corresponding author: Alagan Anpalagan (alagan@ee.ryerson.ca)

ABSTRACT In high-speed digital wireless communication applications, the intersymbol interference channel may have spectral nulls or erasures, which may degrade the orthogonal frequency division multiplexing (OFDM) bit error rate (BER) performance. In this paper, we prove that the BER performance of the OFDM system is considerably refined if the erased symbols in erasure channel (or received symbols on the deep-faded subcarriers in Rayleigh fading channel) are estimated based on the rest symbols in each OFDM signal. Also, an oversampled OFDM scheme which is a particular form of the pre-coded OFDM schemes is considered to guarantee high enough sampling rate. Furthermore, a new iterative receiver is proposed for perfect symbol recovery. A comprehensive Monte Carlo simulation study is performed to validate the theoretical results and affirm the superior performance of the oversampled OFDM scheme with the iterative receiver, compared with the typical detector for the OFDM scheme.

INDEX TERMS Orthogonal frequency division multiplexing (OFDM), intersymbol interference (ISI), erasure channel.

I. INTRODUCTION

Diverse wireless applications draw a lot of attention to orthogonal frequency division multiplexing (OFDM) technique for its straightforward digital accomplishment with IFFT/FFT pairs, and for its endurance against frequency selectivity in wireless channels [1]–[5]. Frequency selective channel in OFDM schemes interchanges into a set of flat fading channels, which can be counteracted by easily applying a one tap equalizer in the frequency domain. However, in more generic linear channels, the precondition for symmetric convolution is not fulfilled and the channel cannot be simply compensated by simple single-tap equalizers, e.g. when the channel has nulls [6], [7] and thus, trustworthy detection of symbols on these subchannels would be severe. This work investigates the issues on detection of symbols on the presence of channel spectral nulls and the erasure channel.

A. LITERATURE REVIEW

Several methods of OFDM symbol recovery and channel estimation have been proposed [8]–[11]. One approach is the data-aided framework, where pilot signals are uniformly interleaved among information symbols and used to estimate channel frequency response at pilot subcarriers [12]–[15]. Another approach is the adaptive bit loading [16]–[18], in which symbols are adaptively transmitted on the subcarriers with high SNRs. The need for feedback at the transmit side confines the adaptive loading efficiency in empirical applications. Subspace detection technique for single carrier transmission with unique words (UW) has been proposed in [19]. Based on the UW structure, the noise subspace is compensated by known training sequences, simplifying data recovery without feedback from the receiver to the transmitter. A multicarrier system with message-driven idle subcarriers (MC-MDIS) has been introduced in [20] for power efficiency and higher spectral compared with OFDM. Alternatively, coded-OFDM (COFDM) [21]–[23] has been proposed to combat channel nulls. The critical dilemma in coding for an OFDM scheme with a large number of subcarriers is that it, either encounters design difficulties or the coding rate becomes prohibitively low. Fundamentally, there are three kind of OFDM-based transmission systems: zero padding OFDM (ZP-OFDM) [24], cyclic prefix OFDM

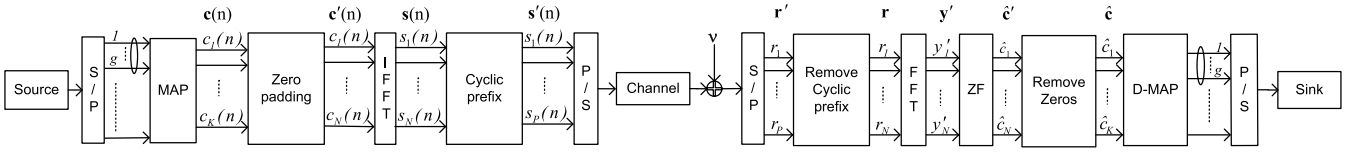

FIGURE 1. Oversampled OFDM system model.

(CP-OFDM) [25], and time domain synchronous OFDM (TDS-OFDM) [26], [27]. TDS-OFDM surpasses ZP-OFDM and CP-OFDM in spectral efficiency. However, the main impediment of TDS-OFDM is that the OFDM data blocks will result in inter block interference (IBI). In this paper, our proposed OFDM scheme uses cyclic prefix instead of zero padding since the CP allow greater resistance for timing errors than the ZP [28].

B. OUR CONTRIBUTION

Oversampled CP-OFDM scheme, a particular one of the redundant pre-coded OFDM schemes [29]–[31] is utilized in this paper. Oversampled CP-OFDM scheme [32]–[36] is acquired by putting some zeros at the tail end of the modulated symbols block, just before the IFFT function at the OFDM transmitter. The first implementation of oversampling for reconstruction of damaged symbols in each CP-OFDM signal has been proposed in [34], where no systematic results have been given in the matter of the error-rate performance and the detection method. Furthermore, unreal Rayleigh channel model conditions have been considered for simplicity in [35] and [36]; however, simulation results and analysis for the erasure channel have not been presented.

The oversampling has other advantages as well, such as enhancing the performance of linear equalizers [32], [37], [38], decreasing OFDM edge effects [39], [40], increasing the time resolution in DFT-based schemes [41], easing the DAC design [33], achieving blind carrier-frequency-offset recovery [42], detection and channel estimation [43], [44], and clipping noise suppression [45].

In this paper, we employ the oversampling to repair the impaired symbols in each OFDM signal from the remaining symbols of the signal, as long as the average rate of the remaining symbols stays above the Nyquist rate. To reconstruct the missing samples from the remaining ones different schemes have been proposed. Some of these schemes use techniques such as convex optimization algorithms [46], a series of filtering process [47], canonical transform [48], matrix-based projections [49], and compressive sensing [50]. For reconstruction of weak symbols in this paper, a novel iterative receiver for OFDM symbol estimation is proposed. The recommended iterative receiver comprises three blocks, namely, non-uniform sampling, low pass filtering, and iterative reconstruction. Furthermore, the closed form end-to-end formulation of the oversampled OFDM scheme employing the iterative reconstruction algorithm is obtained in this paper. Also, the symbol error rate (SER) of our proposed scenario is analytically presented.

The reminder of this paper is arranged as follows. In Section II, the oversampled OFDM scheme that uses standard equalizer in frequency domain is reviewed. The oversampled post-coded OFDM scheme is described in Section III. In this section, erasure subcarriers are modelled in each OFDM frame via the time domain post-coding. To reconstruct the impaired symbols in each OFDM signal, the iterative receiver working based on the non-uniform sampling theorem is described in Section IV. Section V consists of the error probability analysis for the iterative receiver. Section VI gives simulation results, and the paper is concluded in Section VII.

Notation: Throughout this paper, boldface letters denote matrices and column vectors; $\mathbf{0}$ denotes the zero matrix of arbitrary size; $\mathbf{F}_N$ denotes the $N \times N$ discrete Fourier transform (DFT) matrix whose $(n+1, k+1)$th entry is $\exp(-j2\pi nk/N)/\sqrt{N}$; $(.)^{-1}$, $(.)^H$, $(.)^T$, $(.)^\dagger$, and $\|.\|_p$ denote the matrix inversion, conjugate transpose, transpose, Moore-Penrose matrix inversion, and l_p norm operation, respectively; $a_{k,j}$ denotes the (k,j)th entry of the matrix $\mathbf{A}$; Finally, Tr{.} and $E\{.\}$ are trace and expectation operators, respectively.

II. OVERSAMPLED OFDM SCHEME WITH FREQUENCY DOMAIN EQUALIZATION

A. TRANSMITTER

In oversampled OFDM scheme shown in Fig. 1, each block of 2^g modulated symbols in parallel form with size K, $\mathbf{c}(n) = [c_1(n), c_2(n), \ldots, c_K(n)]^T$, zero-padded by inserting $(L-1)K$ zeros at the end of the primary block $\mathbf{c}(n)$ for oversampling before taking IFFT at the transmitter where g is the $\log_2$ of the constellation size in each 2^g modulated symbol, such as 16PSK, 64QAM, etc, and $\mathbf{c}(n)$ is a $K \times 1$ complex column vector in the frequency domain with n as the block index. The m^{th} symbol in the OFDM block that is obtained after utilizing an $N-$point IFFT to $\mathbf{c}'(n) = [c_1(n), c_2(n), \ldots, c_K(n), 0, \ldots, 0]^T$, is:

$$s_m(n) = \frac{1}{\sqrt{N}} \sum_{k=1}^{N} c_k(n) e^{j2\pi k\left(\frac{m}{N}\right)} \quad m = 1, 2, \ldots, N, \quad (1)$$

in which $\mathbf{s}(n) = [s_1(n), s_2(n), \ldots, s_N(n)]^T$ is a DFT coded form of $\mathbf{c}(n)$. It is proved, see [51], [52], that the oversampling in the DFT domain is a Reed-Solomon code capable of correcting $(L-1)K = N-K$ erasures in real field. Note that L is the oversampling factor and regarding the standard OFDM scheme, $L = 1$, is akin to the Nyquist symbol rate. The relationship between the oversampling factor and the out of

band leakage. Also, the out of band leakage, a serious issue in practical systems, decreases when more oversampling factor is considered.

B. RECEIVER

The DFT code, $\mathbf{s}(n)$, is transmitted via a channel after sticking a CP with length no shorter than the channel order. The assumed channel is quasi-static frequency selective Rayleigh fading, therefore the index n can be ignored. Also, $N \times 1$ additive white Gaussian noise (AWGN) vector of $\mathbf{v} = [v_1, v_2, \ldots, v_N]^T$ is added to the signal at the receiver. After discarding the samples of the CP, the signal at the receiver after $N-$point FFT demodulator is:

$$\mathbf{y}' = \Gamma \mathbf{c}' + \mathbf{F}_N \mathbf{v} = \Gamma \mathbf{c}' + \widetilde{\mathbf{v}}, \tag{2}$$

in which $\Gamma = \text{diag}(\mathbf{F}_N \mathbf{h}) = \text{diag}(\Gamma_1, \Gamma_2, \ldots, \Gamma_N)$, is the channel in the frequency domain a diagonal matrix with diagonal elements $\Gamma_1, \Gamma_2, \ldots, \Gamma_N$. The connection of L_h channel taps, $\{h(l)\}_{l=1}^{L_h}$, and $N - L_h$ zeros results in the $\mathbf{h}$. Also, the $\widetilde{\mathbf{v}}$ and $\mathbf{v}$ are $N \times 1$ AWGN noise vectors after and before the FFT process at the receive side, respectively. The estimation of $\widehat{\mathbf{c}'}$ on $\mathbf{c}'$ using the Zero Forcing (ZF) scheme for the symbol recovery is

$$\widehat{\mathbf{c}'} = \Gamma^{-1}\mathbf{y}' = \mathbf{c}' + \Gamma^{-1}\widetilde{\mathbf{v}} = \mathbf{c}' + \mathbf{n}. \tag{3}$$

1) SYMBOL RECOVERY IN NOISELESS CHANNEL

Assuming that the perfect channel state information (CSI) is known only to the receiver, the recovery of $(L-1)K$ erasures per OFDM symbol in noiseless channel is guaranteed by (3).

2) SYMBOL RECOVERY IN NOISY CHANNEL

From (2) and (3), $\mathbf{n} = \Gamma^{-1}\widetilde{\mathbf{v}} = \Gamma^{-1}\mathbf{F}_N\mathbf{v} = \Gamma^{-1}\mathbf{F}_N[\mathbf{v}_{noise} \quad \mathbf{v}_{erasure}]^T$, in which $\mathbf{v}_{noise}$ is $1 \times K$ vector where each element is zero mean AWGN noise with variance σ_v^2 and $\mathbf{v}_{erasure}$ is $1 \times (N-K)$ erasure vector associated to the zero padded positions of oversampled OFDM signal, $\mathbf{c}'$. $\mathbf{v}_{erasure}$ can be set to zero at the receive side and we have $\mathbf{v}' = [\mathbf{v}_{noise} \quad \mathbf{0}]^T$. Therefore, the noise would be $\mathbf{n}' = \Gamma^{-1}\mathbf{F}_N\mathbf{v}'$ with mean 0 and the correlation matrix that can be obtained from

$$\begin{aligned} &E\{\mathbf{n}'\mathbf{n}'^H\} \\ &= \Gamma^{-1}\mathbf{F}_N E\{\mathbf{v}'\mathbf{v}'^H\}\mathbf{F}_N^H \left(\Gamma^{-1}\right)^H \\ &= \Gamma^{-1}\mathbf{F}_N \text{diag}\left(\sigma_v^2, \sigma_v^2, \ldots, \sigma_v^2, 0, \ldots, 0\right)\mathbf{F}_N^H \left(\Gamma^{-1}\right)^H. \end{aligned} \tag{4}$$

Proposition 1: The mth subchannel noise variance of $\mathbf{n}$*, an approximated version of* $\mathbf{n}'$*, is given as*

$$E\{([\mathbf{n}]_m)^2\} \approx \frac{K\sigma_v^2}{N\,|\Gamma_m|^2} \quad m = 1, 2, \ldots, N. \tag{5}$$

Proof: The proof is provided in Appendix A. □

The m^{th} entry of $\mathbf{n}'$ would be amplified to infinity if channel has spectral nulls, i.e., $|\Gamma_m| \approx 0$. Therefore, from (3) all symbols in $\widehat{\mathbf{c}'}$ could not be recovered when channel has nulls.

C. SYMBOL ERROR RATE ANALYSIS OF THE OVERSAMPLED OFDM SCHEME WITH ZF EQUALIZATION

Supposing the modulation scheme QPSK, and modulation symbols $c_k = \pm\sqrt{\varepsilon_c/2} \pm j\sqrt{\varepsilon_c/2}$ with symbol energy ε_c, and $L = 1$ that means the standard OFDM scheme, the SER of the mth subchannel without oversampling is given by [53]:

$$P_{SER}(m) = \frac{1}{2}\left(1 - \left[1 - Q\left(\sqrt{\frac{\varepsilon_c}{\sigma_{v_m}^2}}\right)\right]^2\right), \tag{6}$$

where $\sigma_{v_m}^2$ is the noise variance of the mth subchannel for the standard OFDM scheme, $Q(y) = \frac{1}{\sqrt{2\pi}}\int_y^\infty e^{\frac{-x^2}{2}}dx$, $y \geqslant 0$ is the Gaussian Q-function. Hence, the average SER is

$$P_{SER} = \frac{1}{2K}\sum_{m=1}^{K}\left(1 - \left[1 - Q\left(\sqrt{\frac{\varepsilon_c}{\sigma_{v_m}^2}}\right)\right]^2\right). \tag{7}$$

Similar to the steps in obtaining equation (7), the SER for the oversampled OFDM scheme with respect to the variance of $\mathbf{n}$ in (5) becomes

$$P_{SER} \approx \frac{1}{2LK}\sum_{m=1}^{LK}\left(1 - \left[1 - Q\left(\sqrt{\frac{\varepsilon_c L\,|\Gamma_m|^2}{\sigma_v^2}}\right)\right]^2\right). \tag{8}$$

III. OVERSAMPLED OFDM SCHEME IN ERASURE CHANNEL

The OFDM symbol recovery in the presence of the erasure channel is possible if we use the iterative reconstruction algorithm. In order to understand the performance improvements achieved from the iterative receiver, erasures are assumed to be inserted in each OFDM symbol by means of a simple diagonal matrix. By time domain puncturing of each OFDM symbol, this diagonal matrix results in a channel with spectral nulls. The creation of erasure channel via the simple $N \times N$ puncturing matrix $\mathbf{G}_t = \text{diag}(g_{t1}, \ldots, g_{tN})$, $g_{ti} \in \{0, 1\}$ at the transmitter of Fig. 2, left bottom, is depicted. Henceforth, we show that the time domain puncturing matrix can be modelled as a part of a channel with spectral nulls. For this modelling, we first transform the matrix of $\mathbf{G}_t$ into the frequency domain form and then the effect of this frequency domain version of $\mathbf{G}_t$ in channel model will be precisely described.

At the transmitter, shown in Fig. 2, we have a post-coded OFDM scheme [54] with $\mathbf{G}_t$ as its post-coder. Note that Shah and Tewfik [54] limit the structure design of $\mathbf{G}_f$ based on the bandwidth efficiency, Euclidean distance, and low computational complexity criteria. It is straightforward to show that the post-coding scheme (Fig. 2, left bottom) is equivalent to a pre-coding scheme (Fig. 2, left top) by selecting $\mathbf{G}_f$ as follows:

$$\left.\begin{aligned} \mathbf{s} &= \mathbf{G}_t\mathbf{F}_N^H\mathbf{c}' \\ \mathbf{s} &= \mathbf{F}_N^H\mathbf{G}_f\mathbf{c}' \end{aligned}\right\} \Rightarrow \mathbf{G}_f = \mathbf{F}_N\mathbf{G}_t\mathbf{F}_N^H, \tag{9}$$

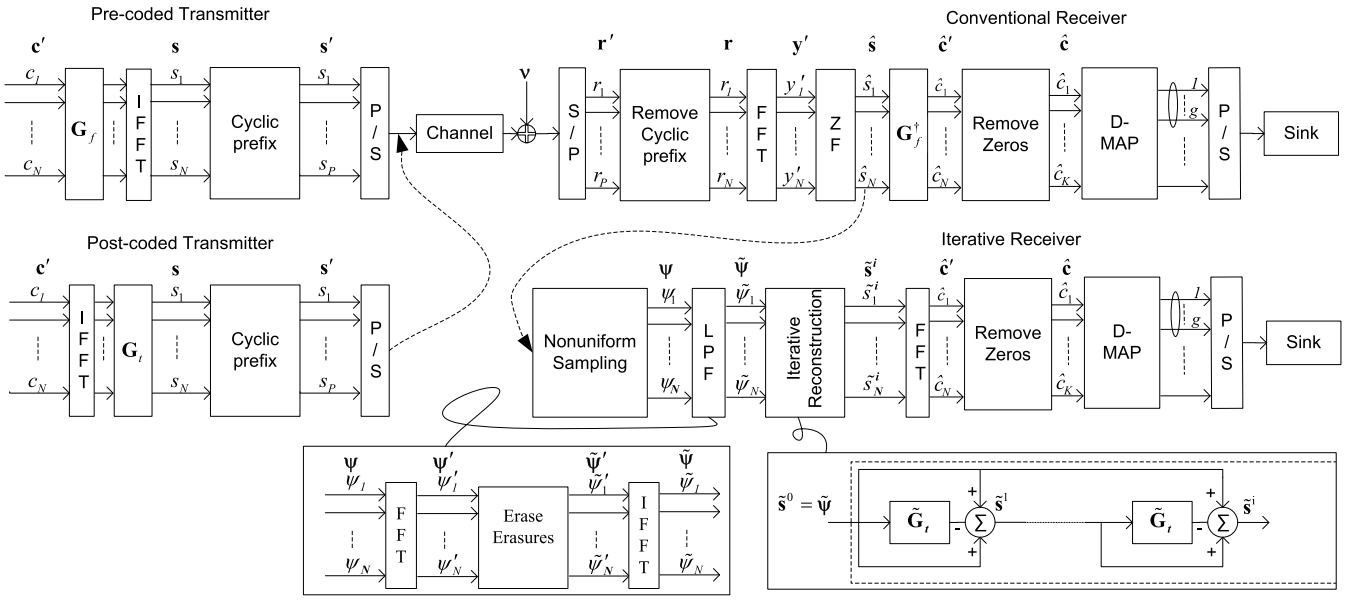

FIGURE 2. The traditional, and the iterative receiver OFDM schemes including post-coded and its equivalent pre-coded transmitter.

TABLE 1. computational complexity for various functions in post-coded and precoded OFDM systems.

	post-coded OFDM [54] (full spreading)	post-coded OFDM [54] (partial spreading $N = MQ$)	Proposed system (with $\uparrow L = 1$)	Precoded OFDM with Zero forcing
FFT	$\mathcal{O}(N\,logN)$	$\mathcal{O}(N\,logN)$	$\mathcal{O}(N\,logN)$	$\mathcal{O}(NL\,logNL)$
IFFT	$\mathcal{O}(NL\,logN)$	$\mathcal{O}(NL\,logN)$	$\mathcal{O}(N\,logN)$	$\mathcal{O}(NL\,logNL)$
Encoding	$\mathcal{O}(N)$	$\mathcal{O}(N)$	$\mathcal{O}(N)$	$\mathcal{O}(N^2L)$
Detection	$\mathcal{O}(N^{3.5})$	$\mathcal{O}(QM^{3.5})$	$\mathcal{O}(N^2)$	$\mathcal{O}(N^3)$

where $\mathbf{G}_f$ is a frequency domain pre-coding matrix. Note that $\mathbf{G}_f$ is a circulant matrix due to the FFT processing on the diagonal matrix $\mathbf{G}_t$ [55]. Also, $\mathbf{G}_f$ is a singular matrix due to the special structure of the diagonal matrix $\mathbf{G}_t$ with entries $g_{ti} \in \{0, 1\}$. $\mathbf{G}_t$ in modelling of erasure channel in this paper is one of the realization of spreading codes $\mathbf{G}_t = diag(\mathbf{F}_N^H \mathbf{c})$ (see [54, eq. (17)]) with bandwidth efficiency, constant Euclidean distance, and low computational complexity in practical wireless communication systems. This means that transmitting an OFDM symbol in erasure channel can be simply modelled with a post-coded OFDM with $\uparrow L = 1$. Therefore, for the first time we could model an erasure channel with a simple post-coded OFDM system with upsampling[1] $\uparrow L = 1$, in this paper. The computation complexity of the system proposed in [54] and our system is compared in Table 1. In pre-coded OFDM partial spreading, the data symbols are spread across Q distinct groups of M subcarrier. Note that our proposed OFDM system has the lower implementation cost.

Considering the transmitting block of Fig. 2, left top (or equivalently the block Fig. 2, left bottom) and the traditional receiver in Fig. 2, right top, the signal after $N-$point FFT demodulator is

$$\mathbf{y}' = \Gamma \mathbf{G}_f \mathbf{c}' + \mathbf{F}_N \mathbf{v}. \tag{10}$$

Note that the term $\Gamma\mathbf{G}_f$ in (10) can be considered as the overall channel model, between $\mathbf{c}'$ and $\mathbf{y}'$, with spectral nulls due to the singular matrix $\mathbf{G}_f$. Due to CP insertion between adjacent information blocks at the transmitter, Γ is a diagonal matrix and its effects can be removed via a simple matrix inversion in ZF block as follows

$$\widehat{\mathbf{s}} = \mathbf{G}_f \mathbf{c}' + \Gamma^{-1} \mathbf{F}_N \mathbf{v}. \tag{11}$$

The issue to be addressed is determining the inverse of the system, i.e., to find the input $\mathbf{c}'$ on spectral nulls given the output signal $\mathbf{G}_f\mathbf{c}'$. The zero-forcing (ZF) equalizer, $\mathbf{G}_f^{\dagger}$, is cascaded at the end of the traditional receiver Fig. 2, as a simple solution for this problem. Unluckily, $N \times N$ matrix inverse of $\mathbf{G}_f$ is necessary for the direct ZF scheme and the computational complexity grow awfully high when N is large. In stark contrast, iterative schemes that are less sensitive to numerical errors, could be useful in manipulating large matrices as mentioned in literature. Henceforth, based on the non-uniform sampling theory, we propose a scheme to discard the damaged symbols in each OFDM signal and iteratively recover the missing symbols from the remaining ones. It will be analytically proved that the proposed scheme would

[1] In [54] upsampling comes from repetitive coding happens due to the smaller size of IFFT process in post-coded OFDM, that is different from the oversampling process in this paper. Oversampled OFDM scheme is acquired by inserting some zeros at the end of the block of the modulated symbols, before the IFFT function.

converge to the $\mathbf{G}_f^{\dagger}$. This shows that the OFDM symbol recovery would be possible in iterative reconstruction algorithm if the non-uniform sampling theorem is guaranteed. Also, note that since $\mathbf{G}_f$ is circulant, it will cause energy leakage across subcarriers. This interference is compensated using the proposed iterative technique as proved in Appendix C.

IV. ITERATIVE RECEIVER

The proposed receiver has three stages: non-uniform sampling, low-pass filtering, and iterative recovery scheme. Fig. 2, right bottom, reveals the iterative receiver for the oversampled OFDM scheme.

A. NONUNIFORM SAMPLING

The input vector of the non-uniform sampling block in Fig. 2 is given in (11). This is obtained through discarding the interference between different symbols via the traditional ZF equalization and de-rotation channel phases in the received OFDM symbol $\mathbf{y}'$. Note that samples in $\widehat{\mathbf{s}}$ may be amplified and cause a high level of noise $\Gamma^{-1}\mathbf{F}_N\mathbf{v}$. To alleviate $\Gamma^{-1}\mathbf{F}_N\mathbf{v}$, symbols in places deliberately set to zero in $\widehat{\mathbf{s}}$ can be discarded and these missing symbols can be recovered from the remaining symbols in each OFDM signal. Note that due to the puncturing matrix $\mathbf{G}_t$, introduced in section III, the positions of time domain punctured samples are known at the receiver. Discarding these punctured samples in each OFDM signal results in a non-uniform sampled version of OFDM signal and perfect signal recovery would be possible as long as the average rate of this signal stays above the Nyquist rate, as the sampling theorem declares. For this, the frequency domain signal $\widehat{\mathbf{s}}$ is transferred to the time domain through the IFFT processing. Then, the puncturing matrix of $\mathbf{G}_t$ is multiplied by $\mathbf{F_N^H}\widehat{\mathbf{s}}$. Non-uniform sampling stage can be briefly expressed as:

$$\mathbf{\Psi} = \mathbf{G}_t\mathbf{F}_N^H\widehat{\mathbf{s}}, \tag{12}$$

B. LOW-PASS FILTERING

To remove a part of high level of noise $\Gamma^{-1}\mathbf{F}_N\mathbf{v}$, low-pass filtering (LPF) process (LPF block in Fig. 2) can be applied. Low pass filtering removes erasures known at the receiver, by using the (N, K) DFT code, expressed as follows. After non-uniform sampling in (12), the signal is processed through FFT operation which provides the below frequency domain signal

$$\mathbf{\Psi}' = \mathbf{F}_N\mathbf{\Psi} = \left[\Psi'_1, \Psi'_2, \ldots, \Psi'_K, \underbrace{\widehat{\Psi}'_{K+1}, \ldots, \widehat{\Psi}'_N}_{Erasures}\right]^T. \tag{13}$$

putting erasures which are known at the receiver to zero, we have $\widetilde{\mathbf{\Psi}'} = \left[\Psi'_1, \Psi'_2, \ldots, \Psi'_K, \underbrace{0, \ldots, 0}_{Erasures}\right]^T$, that diminishes a part of high level of noise $\Gamma^{-1}\mathbf{F}_N\mathbf{v}$. After that, the IFFT process is performed

$$\widetilde{\mathbf{\Psi}} = \mathbf{F}_N^H\widetilde{\mathbf{\Psi}'} = [\widetilde{\Psi}_1, \widetilde{\Psi}_2, \ldots, \widetilde{\Psi}_N]^T. \tag{14}$$

where $\widetilde{\mathbf{\Psi}}$ is a $N \times 1$ complex column vector, with non zero elements.

Equation (14) can be concisely written as:

$$\widetilde{\mathbf{\Psi}} = \mathbf{F}_N^H\mathbf{E}\mathbf{F}_N\mathbf{\Psi}, \tag{15}$$

where $\mathbf{E} = \text{diag}([\mathbf{I}_K\ \mathbf{0}_{N-K}])$, is the erasure matrix. The overall process can be summarized as:

$$\tilde{\Psi} = \mathbf{F}_N^H\mathbf{E}\mathbf{F}_N\mathbf{G}_t\mathbf{F}_N^H\widehat{\mathbf{s}} = \widetilde{\mathbf{G}}_t\mathbf{F}_N^H\widehat{\mathbf{s}}, \tag{16}$$

where $\widetilde{\mathbf{G}}_t$ is the low-pass filtered version of the time domain puncturing matrix $\mathbf{G}_t$.

C. ITERATIVE RECOVERY SCHEME

Iterative recovery scheme, illustrated in Fig. 2, right bottom, due to its fast convergence can be utilized to perfectly reconstruct each modulated block, $\hat{\mathbf{c}}'$, from its low pass filtered version, $\tilde{\Psi}$. The proposed iterative recovery scheme, a modified version of the natural ones recommended by Marvasti [51] is as follows

$$\begin{cases} \widetilde{\mathbf{s}}^i = \tilde{\Psi} + \left(\mathbf{I}_N - \widetilde{\mathbf{G}}_t\right)\widetilde{\mathbf{s}}^{i-1} & i > 0 \\ \widetilde{\mathbf{s}}^0 = \tilde{\Psi} & i = 0, \end{cases} \tag{17}$$

where $\widetilde{\mathbf{s}}^i$, $\widetilde{\mathbf{s}}^{i-1}$ and $\mathbf{I}_N$ are the recovered signal in i^{th} and $(i-1)^{th}$ iteration, and identity matrix of size N, respectively.

Iterative method used in the iterative reconstruction stage. After a large number of iterations, we have $\widetilde{\mathbf{s}}^i = \widetilde{\mathbf{s}}^{i-1}$. Therefore, the steady state value for $\widetilde{\mathbf{s}}^{\infty}$ is obtained from equation (17) as follows

$$\widetilde{\mathbf{s}}^{\infty} = \widetilde{\mathbf{G}}_t^{\dagger}\widetilde{\mathbf{s}}^0 = (\mathbf{F}_N^H\mathbf{E}\mathbf{F}_N\mathbf{G}_t)^{\dagger}\widetilde{\mathbf{s}}^0. \tag{18}$$

However, by inserting (11) in $\widetilde{\mathbf{s}}^0 = \mathbf{F}_N^H\mathbf{E}\mathbf{F}_N\mathbf{G}_t\mathbf{F}_N^H\widehat{\mathbf{s}}$, we have:

$$\begin{aligned} \widetilde{\mathbf{s}}^0 &= \mathbf{F}_N^H\mathbf{E}\mathbf{F}_N\mathbf{G}_t\mathbf{F}_N^H(\mathbf{G}_f\mathbf{c}' + \Gamma^{-1}\mathbf{F}_N\mathbf{v}) \\ &= \mathbf{F}_N^H\mathbf{E}\mathbf{F}_N\mathbf{F}_N^H\mathbf{G}_f\mathbf{F}_N\mathbf{F}_N^H(\mathbf{G}_f\mathbf{c}' + \Gamma^{-1}\mathbf{F}_N\mathbf{v}) \\ &= \mathbf{F}_N^H\mathbf{E}\mathbf{G}_f\mathbf{c}' + \mathbf{F}_N^H\mathbf{E}\mathbf{G}_f\Gamma^{-1}\mathbf{F}_N\mathbf{v} \end{aligned} \tag{19}$$

where (19) is obtained from $\mathbf{G}_t = \mathbf{F_N^H}\mathbf{G}_f\mathbf{F_N}$, $\mathbf{F_N}\mathbf{F_N^H} = \mathbf{I_N}$, and also that $(\mathbf{G}_f)^l = \mathbf{F_N}(\mathbf{G}_t)^l\mathbf{F_N^H} = \mathbf{F_N}\mathbf{G}_t\mathbf{F_N^H} = \mathbf{G}_f$ for $l = 1, 2, \ldots$ due to $\mathbf{G}_t$ which is diagonal with diagonal entries of $g_{t_m} \in \{0, 1\}$. By substituting (19) in (18), the steady state value is

$$\begin{aligned} \widetilde{\mathbf{s}}^{\infty} &= \left(\mathbf{F}_N^H\mathbf{E}\mathbf{F}_N\mathbf{G}_t\right)^{\dagger}\widetilde{\mathbf{s}}^0 = \left(\mathbf{G}_t^{\dagger}\mathbf{F}_N^H\mathbf{E}^{\dagger}\mathbf{F}_N\right)\widetilde{\mathbf{s}}^0 \\ &= \left(\mathbf{F}_N^H\mathbf{G}_f^{\dagger}\mathbf{F}_N\mathbf{F}_N^H\mathbf{E}^{\dagger}\mathbf{F}_N\right)\widetilde{\mathbf{s}}^0 = \mathbf{F}_N^H\mathbf{c}' + \mathbf{F}_N^H\Gamma^{-1}\mathbf{F}_N\mathbf{v} \end{aligned} \tag{20}$$

The iterative algorithm described in sections IV. A - IV. C is summarized in Algorithm 1.

Finally, the complete estimation of $\hat{\mathbf{c}}'$ at the infinite iteration can be obtained by FFT processing at the last block of the iterative receiver in Fig. 2, as follows

$$\hat{\mathbf{c}}' = \mathbf{c}' + \mathbf{F}_N^H\Gamma^{-1}\mathbf{F}_N\mathbf{v}. \tag{21}$$

Algorithm 1 Iterative reconstruction algorithm

Input: ZF-equalized OFDM vector with nulls, $\widehat{\mathbf{s}}$
puncturing matrix, $\mathbf{G}_t$

Output: estimates transmit vector on spectral nulls $\hat{\mathbf{c}}'$

1: Nonuniform Sampling:
discarding samples on nulls: $\boldsymbol{\Psi} = \mathbf{G}_t\mathbf{F}_N^H\widehat{\mathbf{s}}$
2: Low Pass Filtering:
putting erasures to zero: $\widetilde{\boldsymbol{\Psi}} = \mathbf{F}_N^H\mathbf{E}\mathbf{F}_N\boldsymbol{\Psi}$
3: Iterative Reconstruction:
Initialisation : $\widetilde{\mathbf{s}}^0 \leftarrow \widetilde{\mathbf{G}}_t$
4: **for** $i = 0$ to ∞ **do**
5: $\quad\widetilde{\mathbf{s}}^i = \tilde{\Psi} + \left(\mathbf{I}_N - \widetilde{\mathbf{G}}_t\right)\widetilde{\mathbf{s}}^{i-1}$
6: **end for**
7: **return** $\hat{\mathbf{c}}' = \mathbf{F}_N\widetilde{\mathbf{s}}^{\infty}$

Thus, using the iterative reconstruction block in (17), an indirect method for calculating the $\widetilde{\mathbf{G}}_f^{\dagger}$ and therefore calculation of $\hat{\mathbf{c}}'$ from samples on spectral nulls of $\mathbf{G}_f\mathbf{c}'$ at the infinite iteration is proposed.

D. CLOSED FORM RECEIVER's SYSTEM MODEL

Proposition 2: For arbitrary iteration i, the end-to-end relation between the input $\widehat{\mathbf{s}}$*, and the output of the iterative reconstruction block,* $\widetilde{\mathbf{s}}^i$ *in Fig. 2 is*

$$\widetilde{\mathbf{s}}^i = \left(\mathbf{I}_N - (\mathbf{I}_N - \widetilde{\mathbf{G}}_t)^{i+1}\right)\mathbf{F}_N^H\widehat{\mathbf{s}}. \tag{22}$$

Proof: The proof is provided in Appendix B. □

Therefore, similar to the final step for obtaining (21) from (18) by substituting (11) in (22) and taking N-point FFT from $\widetilde{\mathbf{s}}^i$ we have:

$$\hat{\mathbf{c}}' = \mathbf{F}_N\left(\mathbf{I}_N - (\mathbf{I}_N - \mathbf{F}_N^H\mathbf{E}\mathbf{F}_N\mathbf{G}_t)^{i+1}\right) \times \mathbf{F}_N^H(\mathbf{G}_f\mathbf{c}' + \Gamma^{-1}\mathbf{F}_N\mathbf{v}) \tag{23}$$

which shows the closed form input-output relationship between the input $\mathbf{c}'$, and the recovered signal of $\hat{\mathbf{c}}'$ in Fig. 2. Note that the all processing from (12) to (22) are in time domain and for estimation of the transmitted frequency domain signal $\mathbf{c}'$, we should take FFT at (23). After removal zeros block in Fig. 2, which deletes $(L-1)K$ zero symbols from the end of estimated block $\hat{\mathbf{c}}'$, the $K \times 1$ signal $\hat{\mathbf{c}}$ is

$$\hat{\mathbf{c}} = \left\{\hat{c_1'}, \hat{c_2'}, \ldots, \hat{c_K'}\right\}. \tag{24}$$

V. SYMBOL ERROR RATE ANALYSIS OF THE FREQUENCY DOMAIN NONUNIFORM SAMPLING BASED ITERATIVE RECEIVER

Earlier, we obtained from equation (23) a closed relation between input and output of the proposed oversampled transceiver scheme with frequency domain equalizer, where $\mathbf{E}$ and $\mathbf{G}_t$ are diagonal matrices defined in sections III.A and IV.C, respectively. One can easily see that due to the diagonal entries of g_{ti}, $e_i \in \{0, 1\}$ on $\mathbf{G}_t$ and $\mathbf{E}$, the term of $\mathbf{F}_N^H\mathbf{E}\mathbf{F}_N$ is a Hermitian ($(\mathbf{F}_N^H\mathbf{E}\mathbf{F}_N)^H = (\mathbf{F}_N^H\mathbf{E}\mathbf{F}_N)$), normal ($(\mathbf{F}_N^H\mathbf{E}\mathbf{F}_N)(\mathbf{F}_N^H\mathbf{E}\mathbf{F}_N)^* = (\mathbf{F}_N^H\mathbf{E}\mathbf{F}_N)^*(\mathbf{F}_N^H\mathbf{E}\mathbf{F}_N)$), symmetric ($(\mathbf{F}_N^H\mathbf{E}\mathbf{F}_N)^T = (\mathbf{F}_N^H\mathbf{E}\mathbf{F}_N)$), idempotent ($(\mathbf{F}_N^H\mathbf{E}\mathbf{F}_N)^i = (\mathbf{F}_N^H\mathbf{E}\mathbf{F}_N)$, $i = 1, 2, \ldots$), and circulant matrix. Also, it can be proved that $\left\|\mathbf{F}_N^H\mathbf{E}\mathbf{F}_N\mathbf{G}_t\right\|_p \le 1$, where $\|\mathbf{A}\|_p = \sup_{x\neq 0}\frac{\|\mathbf{A}x\|_p}{\|x\|_p}$ is matrix p-norm, defined in [55]. Although the $(\mathbf{F}_N^H\mathbf{E}\mathbf{F}_N)$ and $\mathbf{G}_t$ benefit from the above mentioned properties, element-wise closed form description of $(\mathbf{I}_N - \mathbf{F}_N^H\mathbf{E}\mathbf{F}_N\mathbf{G}_t)^{i+1}$ which is necessary to obtain the SER has severe computational complexity.

A. SIMPLIFYING THE SYSTEM MODEL

In this section, the complex term of $(\mathbf{I}_N - \mathbf{F}_N^H\mathbf{E}\mathbf{F}_N\mathbf{G}_t)^{i+1}$ in the system model of (23) is simplified.

Lemma 1: (a) If $\mathbf{F}_N^H\mathbf{E}\mathbf{F}_N\mathbf{G}_t \in \mathbb{C}^{n\times n}$ and $\left\|\mathbf{F}_N^H\mathbf{E}\mathbf{F}_N\mathbf{G}_t\right\|_p \le 1$, then $(\mathbf{I}_N - \mathbf{F}_N^H\mathbf{E}\mathbf{F}_N\mathbf{G}_t)$ is nonsingular.

(b)

$$\mathbf{I}_N - (\mathbf{I}_N - \mathbf{F}_N^H\mathbf{E}\mathbf{F}_N\mathbf{G}_t)^{i+1} = \left(\sum_{j=0}^{i}\left(\mathbf{I}_N - \mathbf{F}_N^H\mathbf{E}\mathbf{F}_N\mathbf{G}_t\right)^j\right)\left(\mathbf{F}_N^H\mathbf{E}\mathbf{F}_N\mathbf{G}_t\right) \tag{25}$$

Proof: For 1(a) assume $(\mathbf{I}_N - \mathbf{F}_N^H\mathbf{E}\mathbf{F}_N\mathbf{G}_t)$ is singular. It can be concluded that $(\mathbf{I}_N - \mathbf{F}_N^H\mathbf{E}\mathbf{F}_N\mathbf{G}_t)\mathbf{x} = 0$ for some nonzero $\mathbf{x}$ and $\|\mathbf{x}\|_p = \left\|\mathbf{F}_N^H\mathbf{E}\mathbf{F}_N\mathbf{G}_t\mathbf{x}\right\|_p$ implying that $\left\|\mathbf{F}_N^H\mathbf{E}\mathbf{F}_N\mathbf{G}_t\right\|_p \ge 1$, which clearly shows that a contradiction exists. Thus, $(\mathbf{I}_N - \mathbf{F}_N^H\mathbf{E}\mathbf{F}_N\mathbf{G}_t)$ is a nonsingular matrix and has an inverse function.

To prove 1(b), $\left\|\mathbf{F}_N^H\mathbf{E}\mathbf{F}_N\mathbf{G}_t\right\|_p \le 1$, and therefore for every matrix of $\|\mathbf{A}\|_p \le 1$, $\sum_{j=0}^{i}\mathbf{A}^j = \frac{\mathbf{I}_N - \mathbf{A}^{i+1}}{\mathbf{I}_N - \mathbf{A}}$. □

Lemma 2: $\mathbf{F}_N^H\mathbf{E}\mathbf{F}_N\mathbf{G}_t \in \mathbb{C}^{n\times n}$ is nondefective matrix and it can be decomposed to

$$\mathbf{F}_N^H\mathbf{E}\mathbf{F}_N\mathbf{G}_t = \mathbf{V}\boldsymbol{\Lambda}\mathbf{V}^{-1}, \tag{26}$$

in which eigenvectors and eigenvalues for $\mathbf{F}_N^H\mathbf{E}\mathbf{F}_N\mathbf{G}_t$ are linearly independent columns in the matrix $\mathbf{V}$ and the matrix $\boldsymbol{\Lambda} = \mathrm{diag}(\lambda_1, \lambda_2, \cdots, \lambda_N)$, respectively.

Proof: We can find a nonsingular $\mathbf{V} \in \mathbb{C}^{n\times n}$ with the property that $\mathbf{V}(\mathbf{F}_N^H\mathbf{E}\mathbf{F}_N\mathbf{G}_t)\mathbf{V}^{-1} = \mathrm{diag}(\lambda_1, \lambda_2, \cdots, \lambda_N)$, therefore the matrix of $\mathbf{F}_N^H\mathbf{E}\mathbf{F}_N\mathbf{G}_t$ is diagonalizable or non-defective as defined in [55]. □

Lemma 3: $\mathbf{F}_N^H\mathbf{E}\mathbf{F}_N\mathbf{G}_t$ eigenvalues are real and

$$\mathrm{eig}(\mathbf{I}_N - \mathbf{F}_N^H\mathbf{E}\mathbf{F}_N\mathbf{G}_t) = \mathbf{I}_N - \boldsymbol{\Lambda} \tag{27}$$

$$\left(\mathbf{F}_N^H\mathbf{E}\mathbf{F}_N\mathbf{G}_t\right)^i = \mathbf{V}\boldsymbol{\Lambda}^i\mathbf{V}^{-1} \tag{28}$$

Proof: If $\mathbf{A}$ is a Hermitian matrix with λ_m eigenvalues, then $\mathrm{Tr}\left(\mathbf{A}^i\right) = \sum_m \lambda_m^i$, and $\mathrm{eig}(\mathbf{I}_N - c\mathbf{A}) = 1 - c\lambda_m$ with $\lambda_m \in \mathbb{R}$, as mentioned in [56]. $\mathbf{F}_N^H\mathbf{E}\mathbf{F}_N\mathbf{G}_t$ is Hermitian, and thus the Lemma is proved. □

Theorem 1: For every diagonalizable Hermitian matrix $\mathbf{F}_N^H\mathbf{E}\mathbf{F}_N\mathbf{G}_t \in \mathbb{C}^{n\times n}$, with $\left\|\mathbf{F}_N^H\mathbf{E}\mathbf{F}_N\mathbf{G}_t\right\|_p \le 1$, and $\boldsymbol{\Lambda} = \mathrm{eig}(\mathbf{F}_N^H\mathbf{E}\mathbf{F}_N\mathbf{G}_t)$, we conclude that:

$$\left(\mathbf{I}_N - (\mathbf{I}_N - \mathbf{F}_N^H\mathbf{E}\mathbf{F}_N\mathbf{G}_t)^{i+1}\right) = \mathbf{V}(\mathbf{I}_N - \boldsymbol{\Lambda}'^{i+1})\mathbf{V}^{-1}, \tag{29}$$

in which $\boldsymbol{\Lambda}' = \mathbf{I}_N - \boldsymbol{\Lambda}$.

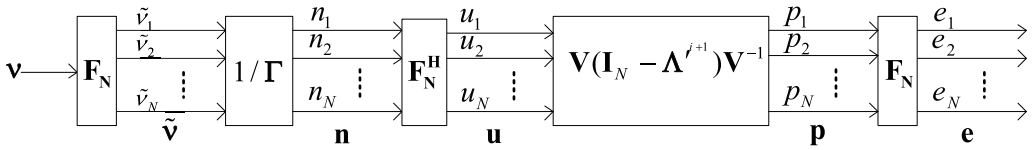

FIGURE 3. Noise path at the proposed iterative receiver.

Proof: From (25)- (28) we deduce that:

$$\begin{aligned}
&\mathbf{I}_N - (\mathbf{I}_N - \mathbf{F}_N^H \mathbf{E} \mathbf{F}_N \mathbf{G}_t)^{i+1} \\
&\quad = \left(\sum_{j=0}^{i} \left(\mathbf{I}_N - \mathbf{F}_N^H \mathbf{E} \mathbf{F}_N \mathbf{G}_t \right)^j \right) \left(\mathbf{F}_N^H \mathbf{E} \mathbf{F}_N \mathbf{G}_t \right) \\
&\quad = \left(\mathbf{V} \sum_{j=0}^{i} (\mathbf{I}_N - \mathbf{\Lambda})^j \mathbf{V}^{-1} \right) \left(\mathbf{V} \mathbf{\Lambda} \mathbf{V}^{-1} \right) \\
&\quad = \mathbf{V} \left(\sum_{j=0}^{i} (\mathbf{I}_N - \mathbf{\Lambda})^j \mathbf{\Lambda} \right) \left(\mathbf{V}^{-1} \right) \\
&\quad = \mathbf{V} (\mathbf{I}_N - \mathbf{\Lambda}'^{i+1}) \mathbf{V}^{-1} \qquad (30)
\end{aligned}$$

where $\mathbf{\Lambda}' = \text{eig}(\mathbf{I}_N - \mathbf{F}_N^H \mathbf{E} \mathbf{F}_N \mathbf{G}_t)$. □

Consequently, the proposed iterative receiver's model for arbitrary iteration i, is easily achieved from a diagonal term $\mathbf{\Lambda}'^{i+1}$ in (30) in place of the computationally complex term $(\mathbf{I}_N - \mathbf{F}_N^H \mathbf{E} \mathbf{F}_N \mathbf{G}_t)^{i+1}$ in (22).

B. SYMBOL ERROR PROBABILITY

To derive the SER of our proposed scheme, we use noise path at the receive side. We assume that $N \times 1$ complex circular AWGN noise $\mathbf{v}$, with variance σ_v^2 for each entry, and QPSK modulation symbols of $c_k = \pm\sqrt{\varepsilon_c/2} \pm j\sqrt{\varepsilon_c/2}$ with ε_c as the symbol energy. In the proposed iterative receiver, the $N \times 1$ noise $\mathbf{e}$ can be examined by the receiver block diagram in Fig. 3. This graph can be validated by equation (23). It is straightforward that the entries in $\mathbf{n}$ are Gaussian random variables with variance $\sigma_{n_j}^2 \approx \frac{K\sigma_v^2}{N|\Gamma_j|^2} \quad j = 1, 2, \ldots, N$. The elements in $\mathbf{u} = \mathbf{F}_N^H \mathbf{n}$ are Gaussian random variables with variance $\sigma_{u_j}^2 = \sigma_{n_j}^2$, because of the unitary feature of $\mathbf{F}_N^H$. Each element in the noise $\mathbf{p}$ can be expressed as

$$p_j = \sum_{m=0}^{N} \left[\mathbf{V}(\mathbf{I}_N - \Lambda'^{i+1}) \mathbf{V}^{-1} \right]_{m,j}^{*} u_m. \qquad (31)$$

Lemma 4: The elements of noise $\mathbf{p}$ are Gaussian random variables, with following approximate variance:

$$\sigma_p^2 \approx E[\bar{\mathbf{p}} \circ \mathbf{p}] = \left\| \mathbf{V}(\mathbf{I}_N - \Lambda'^{i+1}) \mathbf{V}^{-1} \right\|_2 \sigma_{\mathbf{u}}^2 \mathbf{I}_{N \times 1}, \qquad (32)$$

in which $\sigma_{\mathbf{u}}^2 \approx \text{diag}(\sigma_{u_1}^2, \sigma_{u_2}^2, \ldots, \sigma_{u_N}^2)$, $\mathbf{A} \circ \mathbf{B}$ is the Hadamard matrix product which is entry-wise product of two matrices of the same dimensions $[\mathbf{A} \circ \mathbf{B}]_{i,j} = [a_{ij} b_{ij}]$, and $\bar{\mathbf{A}}$ is the component-wise conjugate of $\mathbf{A}$.

TABLE 2. BER of the proposed frequency domain iterative receiver for different coherent modulation schemes.

Modulation	$P_b(\gamma_b)$
QPSK	$\frac{1}{N} \sum_{m=1}^{N} Q\left(\sqrt{\frac{\varepsilon_c}{\sigma_v^2 \sum_{j=1}^{N} 1/\lvert\Gamma_j\rvert^2 \left\| \sum_{t=1}^{N} a_{mt} b_{jt} (1 - \lambda_t'^{i+1}) \right\|_2}} \right)$
MPSK	$\frac{2}{\log_2 M} \times \frac{1}{N} \sum_{m=1}^{N} Q\left(\sqrt{\frac{\varepsilon_c \log_2 M \times \sin^2(\pi/M)}{\sigma_v^2 \sum_{j=1}^{N} 1/\lvert\Gamma_j\rvert^2 \left\| \sum_{t=1}^{N} a_{mt} b_{jt} (1 - \lambda_t'^{i+1}) \right\|_2}} \right)$
MQAM	$\frac{4}{\log_2^M} \left(1 - 1/\sqrt{M}\right) \times \frac{1}{N} \sum_{m=1}^{N} Q\left(\sqrt{\frac{3}{(M-1)} \frac{\varepsilon_c}{\sigma_v^2 \sum_{j=1}^{N} 1/\lvert\Gamma_j\rvert^2 \left\| \sum_{t=1}^{N} a_{mt} b_{jt} (1 - \lambda_t'^{i+1}) \right\|_2}} \right)$

Proof: The proof is provided in Appendix D. □

For each OFDM symbol, the jth subchannel noise variance is $\sigma_{e_j}^2 = \sigma_{p_j}^2$, because of the $\mathbf{F}_N$ unitary feature at the ending block in Fig. 3. Therefore, the SER of the proposed system using the iterative receiver with QPSK signal constellation can be provided by (33), as shown at the bottom of the next page.

C. BIT ERROR RATE

We can expand the results to QAM, PSK, and PAM by using estimates for bit error rate (BER) achieved from SER. We will consider QAM modulation as an instance. The SER for each subchannel can be obtained from the equation (34), as shown at the bottom of the next page, assuming the system of $M-$ary QAM symbols with variance ε_c. BER can be approximated from SER as $P_{BER}(m) \approx {}^{P_{SER}(m)}/_{\log_2^M}$ [53] when Gray code is used. So, the equation (35), as shown at the bottom of the next page, is derived.

Table 2 reveals the BER for some coherent modulation schemes.

D. PERFORMANCE IMPROVEMENT IN RAYLEIGH CHANNEL

Regardless of performance improvement in erasure channel, and the known position of the sample loss and its unknown amplitude, the iterative receiver can be used to alleviate the Rayleigh fading channel nulls. The proposed scheme used for combating the Rayleigh fading channel nulls, which is simpler than the one introduced in section IV, is depicted in Fig. 4. Consider that the CSI is known at the receiver side. Thus, after ZF equalizer at the receiver side, we can drop the frequency domain samples on deep faded subchannels by discarding matrix $\mathbf{O}$ in non-uniform sampling block, as shown in Fig. 4. Then, the lost samples from each OFDM

frame can be recovered by the iterative reconstruction block. The discarding matrix $\mathbf{O} = \text{diag}[O_1, O_2, \ldots, O_N]$, which discards the deep faded symbols of each OFDM symbol, is a $N \times N$ diagonal matrix with $O_i = \begin{cases} 1 & |\Gamma_i| \geq \theta \\ 0 & \text{otherwise} \end{cases}$, where θ is the discarding threshold and $\Gamma = \text{diag}[\Gamma_1, \Gamma_2, \ldots \Gamma_N]$ is the channel vector. Discarding threshold θ, in our proposed scheme, is selected based on the magnitude of entries of channel vector. After dropping deep faded samples on subchannels with magnitude below the discarding threshold θ, the iterative reconstruction block recovers each OFDM frame $\mathbf{\Psi}$. Note that in Fig. 4, $\mathbf{\Psi}$ is the non-uniform sampled vector and $\mathbf{O}$ is the discarding matrix used to produce the $\mathbf{\Psi} = \mathbf{O}\widehat{\mathbf{s}}$. Also, the matrix $\mathbf{O}$ and the vector $\mathbf{\Psi}$ should be substituted for $\widetilde{\mathbf{G}}_t$ and $\widetilde{\mathbf{\Psi}}$ in the iterative reconstruction algorithm in Fig. 2 to be used in Fig. 4, respectively. Hence, the iterative model for reconstructing deep Rayleigh faded subchannels can be written as

$$\begin{cases} \widetilde{\mathbf{s}}^i = \mathbf{\Psi} + (\mathbf{I}_N - \mathbf{O})\widetilde{\mathbf{s}}^{i-1} & i > 0 \\ \widetilde{\mathbf{s}}^0 = \mathbf{\Psi} & i = 0. \end{cases} \tag{36}$$

E. DISCUSSION ON THE SAMPLING LOSS

In erasure channel, the amplitude of the sample loss is unknown; however, its position is known. The memoryless erasure channel is a helpful abstraction for diverse kinds of low reliability reception or data loss, and plays a fundamental role in information theory of noisy channels and channel coding theory. Instances of an erasure channel are the missing of a symbol physically stored in a computer memory or the erased information in video, text, image, and audio applications, and the packet loss in an ATM network. As an illustrative application, the location of the erased symbol is determined by knowing the rest of the text if one of the symbols in a text is erased [57]. If P_ϵ is designated as the sampling loss probability, then $1/1 - P_\epsilon$ is the sampling rate essential for errorless transmission [51]. In Rayleigh fading channel and erasure channel, sample loss appeared in our proposed system due to the discarding matrix $\mathbf{O}$ and the puncturing matrix $\mathbf{G}_t$, respectively. Note that the iterative method diverges for the rates less than the $\frac{1}{1-P_\varepsilon}$. The sampling loss probability at the proposed receiver would be $P_\varepsilon = \frac{n_0}{N}$, if n_0 is defined as the number of zero elements on the diagonal puncturing matrix $\mathbf{G}_t$ (discarding matrix of $\mathbf{O}$) in erasure channel (Rayleigh fading channel). Hence, for error-free transmission, the sampling rate of $\frac{N}{N-n_0}$ should be selected at the transmit side. For putting into practice the oversampling factor of $\frac{N}{N-n_0}$, we can insert $(\frac{N}{N-n_0} - 1)K$ zero samples after each data block of length K. This means that we have an (N, K) code, that with the iterative method is capable of recovering the $N - K = (\frac{N}{N-n_0} - 1)K$ lost samples. This discussion is consistence with notes in II.A.

VI. RESULTS AND DISCUSSION

In this section the performance of the proposed schemes are evaluated through simulation. Unless specified otherwise, the data block's size considering 16QAM modulation on each element is $K = 32$, the number of subcarriers is $N = 128$, the oversampling factor is $L = 4$, and the number of iteration performed at the iterative receiver is $i = 10$. Note that the oversampling factor of $L = \frac{1}{1-P_\varepsilon} = 4$ guarantees errorless communication if $P_\varepsilon = \frac{3}{4}$ of samples are lost.

A. BER PERFORMANCE IN ERASURE CHANNELS

For a given probability of sampling loss, P_ϵ, Figs. 5 - 7 show the BER vs SNR of the proposed iterative receiver for different number of iterations $i = 1, 10, 100$, respectively. The iterative receiver boosts the BER performance significantly as more iterations are repeated in erasure channel. From the figures, it is clear that the numerical results match well with their simulated counterparts, confirming the accuracy of the analysis. Fig. 8 compares the BER performance of the oversampled OFDM system, the (15, 3) Reed Solomon (RS) coded OFDM

$$P_{SER\_QPSK} \approx \frac{1}{N} \times \sum_{m=1}^{N} \left(1 - \left[1 - Q\left(\sqrt{\frac{N\varepsilon_c}{K\sigma_v^2 \sum_{j=1}^{N} 1/|\Gamma_j|^2 \left\| \sum_{t=1}^{N} a_{mt} b_{jt} (1 - \lambda_t^{i+1}) \right\|_2}} \right) \right]^2 \right) \tag{33}$$

$$P_{SER\_MQAM}(m) \approx 4\left(1 - 1/\sqrt{M}\right) \times Q\left(\sqrt{\frac{3}{(M-1)} \frac{N\varepsilon_c}{K\sigma_v^2 \sum_{j=1}^{N} 1/|\Gamma_j|^2 \left\| \sum_{t=1}^{N} a_{mt} b_{jt} (1 - \lambda_t^{i+1}) \right\|_2}} \right) \tag{34}$$

$$P_{BER\_MQAM} \approx \frac{4}{\log_2^M}\left(1 - 1/\sqrt{M}\right) \times \frac{1}{N} \sum_{m=1}^{N} Q\left(\sqrt{\frac{3}{(M-1)} \frac{N\varepsilon_c}{K\sigma_v^2 \sum_{j=1}^{N} 1/|\Gamma_j|^2 \left\| \sum_{t=1}^{N} a_{mt} b_{jt} (1 - \lambda_t^{i+1}) \right\|_2}} \right) \tag{35}$$

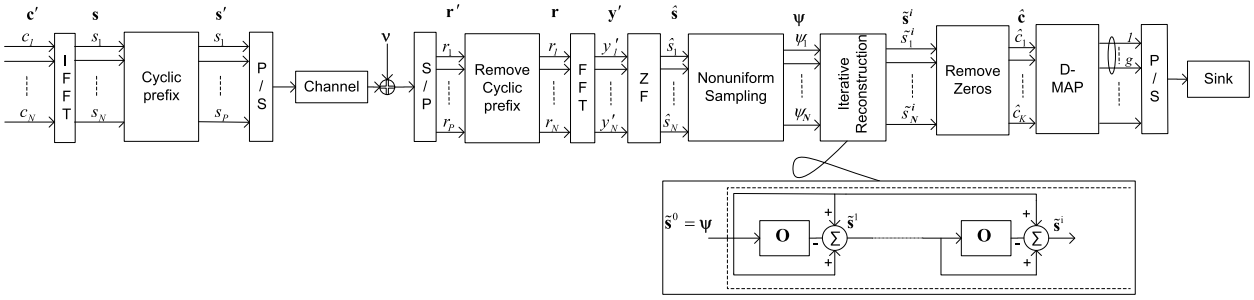

FIGURE 4. The proposed iterative receiver for alleviating the Rayleigh fading channel nulls.

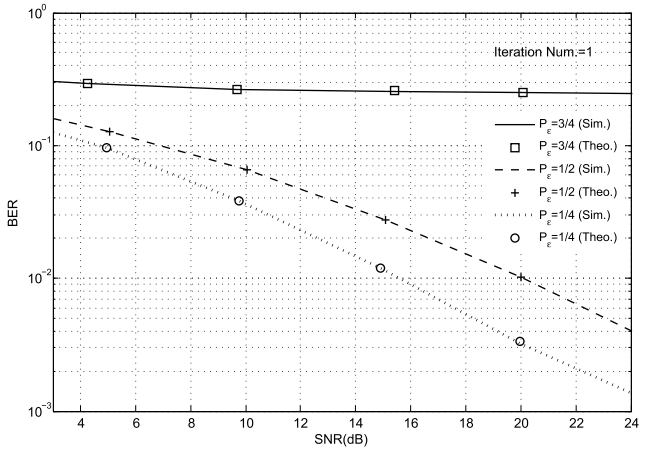

FIGURE 5. BER of the iterative receiver in erasure channel for $P_\epsilon = \frac{1}{4}, \frac{1}{2}, \frac{3}{4}$ and 1 iteration.

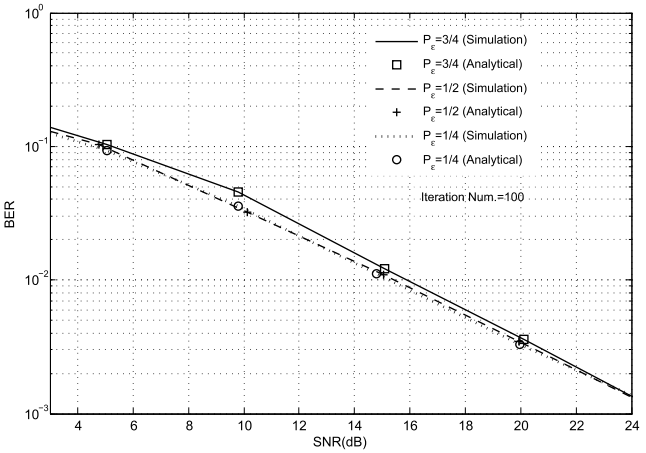

FIGURE 7. BER of the iterative receiver in erasure channel for $P_\epsilon = \frac{1}{4}, \frac{1}{2}, \frac{3}{4}$ and 100 iterations.

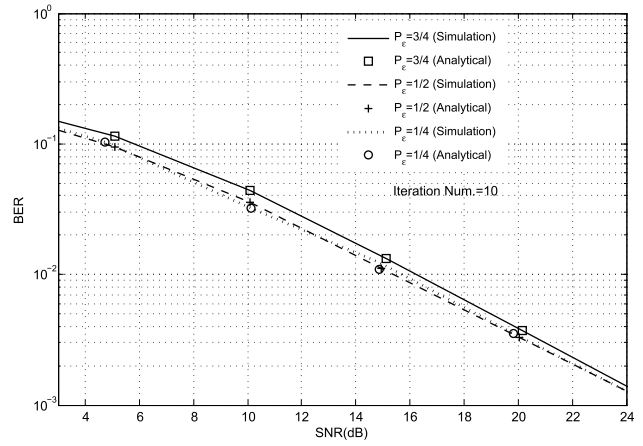

FIGURE 6. BER of the iterative receiver in erasure channel for $P_\epsilon = \frac{1}{4}, \frac{1}{2}, \frac{3}{4}$ and 10 iterations.

system, and the (511, 130) BCH coded OFDM system with the same bandwidth. In (21) and (23), it is analytically proved that $\mathbf{c}'$ can be completely recovered from $\mathbf{s}$ using the convergent iterative receiver. Note that if sufficient redundancy is provided, perfect reconstruction is guaranteed. Therefore, for the sampling loss probability $P_\varepsilon = n_0/N = 15\%$, 25% or 50% assumed in Fig. 8, perfect recovery is ensured with an oversampling factor of $L = 4$. Take into account that the BER performance of (15, 3) RS and (511, 130) BCH coded OFDM systems for the conditions in which 50%, 75%, and 85% of data are transmitted do not converge to the best condition (the curve depicted with + sign) in which 100% of data is transmitted. In other words, the divergence between the BER curve and the one marked with + sign showing the BCH and RS coded OFDM schemes is increased when a smaller amount of data is transmitted. Evidently, the code rate for (15, 3) RS is 1/3 that is bigger than the others, 1/4, and produces stronger code for the condition where 100% of data is transmitted. By way of conclusion, using our proposed receiver including channel coding techniques, e.g., RS/BCH codes will improve the performance of our proposed oversampled OFDM scheme at the expense of more bandwidth and deep interleaver.

B. A NOTE ON CONVERGENCE

It has been proved in [51] that to recover a signal from its non-uniform samples, after a limited number of iterations the iterative method approaches to the desired signal if the power of error signal is lower than the power of the desired one. In this paper, we expect to recover each OFDM block, $\mathbf{c}'$, from its non-uniform samples on spectral nulls, $\tilde{\Psi}$, through the iterative receiver. Therefore, the iterative reconstruction block converges to the desired OFDM symbol after a finite amount

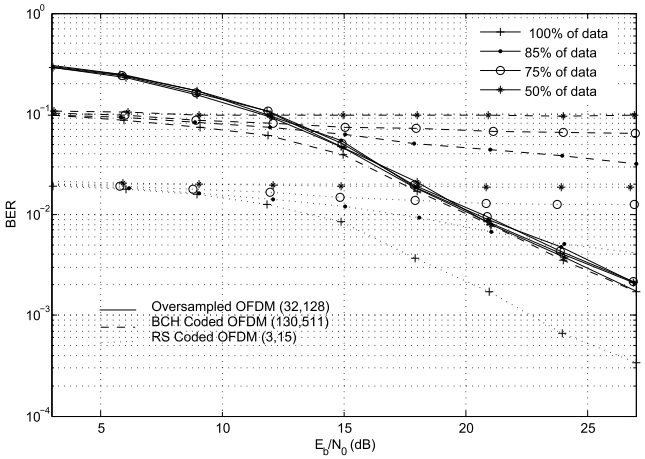

FIGURE 8. BER for (15, 3) RS coded, (511, 130) BCH coded, and the oversampled OFDM system versus E_b/N_0.

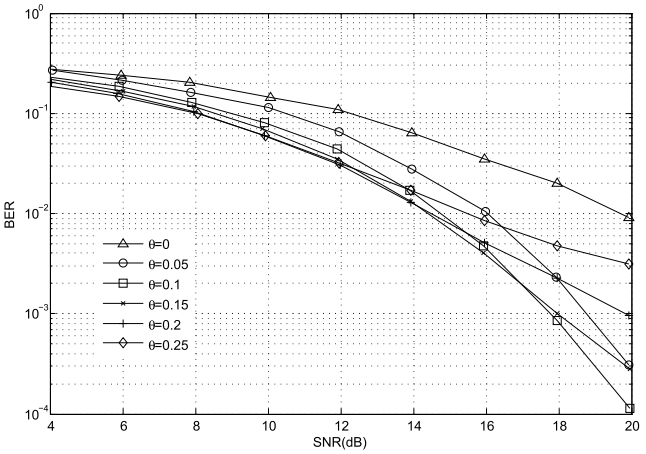

FIGURE 9. BER for the iterative receiver for different values of θ in Rayleigh fading channel.

TABLE 3. Mean-square error for proposed iterative receiver.

Iteration Num.	$P_\epsilon = \frac{3}{4}$	$P_\epsilon = \frac{1}{2}$	$P_\epsilon = \frac{1}{4}$
1	0.6180e-1	0.1221e-1	0.7629e-2
2	0.3476e-3	0.305e-4	0.477e-5
3	0.1955e-3	0.76e-5	0.30e-7
4	0.1100e-3	0.19e-5	0.2e-8
5	0.619e-4	0.5e-6	0.0000
6	0.348e-4	0.1e-6	0.0000
7	0.196e-4	0.0000	0.0000
8	0.110e-4	0.0000	0.0000
9	0.62e-5	0.0000	0.0000
10	0.35e-5	0.0000	0.0000

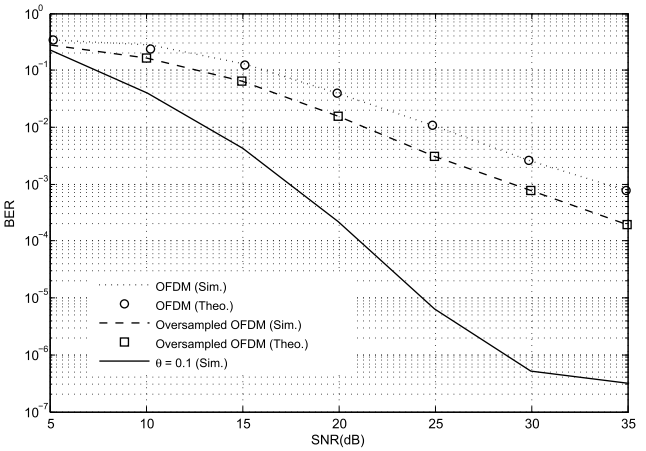

FIGURE 10. BER for the traditional, the non-iterative oversampled and the iterative oversampled with $\theta = 0.1$, OFDM systems in Rayleigh fading channel.

of iterations if the power of the missing symbols in $\tilde{\Psi}$, is lower than the power of the symbols in $\mathbf{c}'$. Note that for the iterations with the values of $i = 10$ and $i = 100$ both BER performances followed a very similar trend in Figs. 6 - 7, which implies fast convergence rate of our proposed receiver. Also, the mean square error for the maximum number of iterations $i = 10$, and with the oversampling factor of $L = 4$ is shown in Table 3. Note that the worst case is $P_\epsilon = \frac{3}{4}$, and for $0 \leq P_\varepsilon < \frac{3}{4}$ with the oversampling factor of $L = 4$, the stopping criterion (a small number around 1e-5) is fulfilled for the lower number of iterations.

C. DISCARDING THRESHOLD OF θ IN OVERSAMPLED OFDM SCHEME

The BER performance of the proposed iterative receiver in Rayleigh fading channel is depicted in Fig. 9. This figure illustrates curves corresponding to different discarding thresholds of $\theta = 0, 0.05, 0.1, 0.15, 0.2, 0.25$ in Rayleigh fading channel. Note that the probability of sampling loss, P_ϵ, in the Rayleigh fading channel depends on the discarding threshold of θ. Obviously, the larger number of high-quality samples results in better BER performance, and we have larger number of these type of samples in high SNR regime. Therefore, in low SNR regime, a higher value for θ should be considered to discard a larger number of low-quality samples in each OFDM symbol. Conversely, In high SNR regime, a smaller value for θ should be considered to discard a smaller number of high-quality samples in each OFDM symbol. Thus, there is a trade-off between θ and the probability of sampling loss in different channel conditions. Also, notice at high SNR regime in Fig. 9, the iterative receiver with $\theta = 0.1$ achieves the best performance in Rayleigh fading channel for the oversampling factor of $L = 4$. The Iterative Receiver for oversampled OFDM system in frequency non selective channel.

D. PERFORMANCE COMPARISON BETWEEN TRADITIONAL RECEIVER AND THE ITERATIVE RECEIVER IN RAYLEIGH CHANNEL

Fig. 10 compares the oversampled OFDM system BER performance with both the iterative ($\theta = 0.1$) and the traditional

receiver versus the non-oversampled OFDM system. Note that the proposed iterative receiver provides a better BER performance rather than the traditional receiver. Specially, at bit error rate 10^{-3}, the iterative receiver achieves a 12.5 dB gain in SNR over the traditional OFDM system. It can also be observed at bit error rate 10^{-3}, the iterative receiver reaps 17.5 dB gain in SNR over the non-oversampled OFDM system.

VII. CONCLUSIONS

An effective OFDM signal recovery method is introduced in this paper. The oversampling is applied at the OFDM transmitter so that the OFDM iterative receiver can perfectly reconstruct the data on spectral nulls or the erased data in Rayleigh fading channel or the Erasure channel, respectively. Without any need for changing or applying extra channel coding at the transmitter, all the processing is performed at the receiver in our proposed system. As stated for the transmission, this can save more bandwidth. Simulation and analytical results show significant BER improvements for the proposed scheme in Erasure channel and Rayleigh fading channel. Furthermore, the need for the low number of iterations and the rapid convergence rate are proved through simulation for the proposed iterative receiver. The analysis of the system in fast fading channel, and the mathematical analysis for the trade-off between L and the sampling loss probability in different channel conditions will be derived in our future work.

APPENDIX A
PROOF OF THE EQUATION (5)

Proof: By expanding the (5) we have:

$$
\begin{aligned}
&E\{\mathbf{n}'\mathbf{n}'^{H}\} \\
&= \mathbf{\Gamma}^{-1}\mathbf{F}_N E\{\mathbf{v}'\mathbf{v}'^{H}\}\mathbf{F}_N^H \left(\mathbf{\Gamma}^{-1}\right)^H \\
&= \begin{pmatrix}
\dfrac{\sigma_v^2}{\Gamma_1 * \Gamma_1^H}\displaystyle\sum_{j=1}^{K} f_{1,j}f_{1,j}^* & \cdots & \dfrac{\sigma_v^2}{\Gamma_1 * \Gamma_N^H}\displaystyle\sum_{j=1}^{K} f_{1,j}f_{N,j}^* \\
\vdots & \ddots & \vdots \\
\dfrac{\sigma_v^2}{\Gamma_N * \Gamma_1^H}\displaystyle\sum_{j=1}^{K} f_{N,j}f_{1,j}^* & \cdots & \dfrac{\sigma_v^2}{\Gamma_N * \Gamma_N^H}\displaystyle\sum_{j=1}^{K} f_{N,j}f_{N,j}^*
\end{pmatrix} \\
&= \begin{pmatrix}
K\sigma_v^2/N \,\|\Gamma_1\|^2 & & 0 \\
& \ddots & \\
0 & & K\sigma_v^2/N \,\|\Gamma_N\|^2
\end{pmatrix} \qquad (37)
\end{aligned}
$$

where the last equality is concluded from $\mathbf{F}_N \times \mathbf{F}_N^H = I_N \Rightarrow \sum_{j=1}^{N} f_{i,j}f_{i,j}^* = \begin{cases} 1 & i = j \\ 0 & i \neq j \end{cases}$.

Note that $\mathbf{n}'$ is an approximated version of $\mathbf{n} = \Gamma^{-1}\mathbf{F}_N[\mathbf{v}_{noise} \quad \mathbf{v}_{erasure}]^T$ by setting the erasure vector $\mathbf{v}_{erasure}$ to zero; thus $\sigma_{\mathbf{n}}^2 \approx \sigma_{\mathbf{n}'}^2$. □

APPENDIX B
PROOF OF THE EQUATION (22)

We obtain the input-output relation of our proposed iterative receiver in Fig. 2 for any arbitrary iteration i as described as follows. We define the error vector as $\mathbf{e}_i = \widetilde{\mathbf{s}}^i - \widetilde{\mathbf{G}}_t^{\dagger}\widetilde{\mathbf{s}}^0$. Subtracting the equation (17) from the true solution $\widetilde{\mathbf{G}}_t^{\dagger}\widetilde{\mathbf{s}}^0$, the error at step i is derived as:

$$
\begin{aligned}
\mathbf{e}_i &= (\mathbf{I}_N - \widetilde{\mathbf{G}}_t)\mathbf{e}_{i-1} \\
&= \ldots = (\mathbf{I}_N - \widetilde{\mathbf{G}}_t)^i \mathbf{e}_0 \qquad (38) \\
\Rightarrow \mathbf{e}_0 - \mathbf{e}_i &= \left(\mathbf{I}_N - (\mathbf{I}_N - \widetilde{\mathbf{G}}_t)^i\right)\mathbf{e}_0 \\
&= \left[\sum_{j=1}^{i}\binom{i}{j}(-1)^{j-1}\widetilde{\mathbf{G}}_t^j\right]\mathbf{e}_0 \qquad (39)
\end{aligned}
$$

Therefore, the closed form input-output formula for the proposed iterative receiver can be derived as follows:

$$
\begin{aligned}
\mathbf{e}_0 - \mathbf{e}_i &= \widetilde{\mathbf{s}}^0 - \widetilde{\mathbf{s}}^i = \left(\mathbf{I}_N - (\mathbf{I}_N - \widetilde{\mathbf{G}}_t)^i\right)\left(\widetilde{\mathbf{s}}^0 - \widetilde{\mathbf{G}}_t^{\dagger}\widetilde{\mathbf{s}}^0\right) \\
&\Rightarrow \widetilde{\mathbf{s}}^i = \widetilde{\mathbf{s}}^0 - (\mathbf{e}_0 - \mathbf{e}_i) \\
&= \widetilde{\mathbf{s}}^0 - \left(\mathbf{I}_N - (\mathbf{I}_N - \widetilde{\mathbf{G}}_t)^i\right) \\
&\quad \times \left(\widetilde{\mathbf{s}}^0 - \widetilde{\mathbf{G}}_t^{\dagger}\widetilde{\mathbf{s}}^0\right) \\
&= \widetilde{\mathbf{s}}^0 - \left(\widetilde{\mathbf{s}}^0 - \widetilde{\mathbf{G}}_t^{\dagger}\widetilde{\mathbf{s}}^0 - (\mathbf{I}_N - \widetilde{\mathbf{G}}_t)^i\left(\widetilde{\mathbf{s}}^0 - \widetilde{\mathbf{G}}_t^{\dagger}\widetilde{\mathbf{s}}^0\right)\right) \\
&\Rightarrow \widetilde{\mathbf{s}}^i = \left(\widetilde{\mathbf{G}}_t^{\dagger} - (\mathbf{I}_N - \widetilde{\mathbf{G}}_t)^i(\widetilde{\mathbf{G}}_t^{\dagger} - \mathbf{I}_N)\right)\widetilde{\mathbf{s}}^0. \qquad (40)
\end{aligned}
$$

$\widetilde{\mathbf{s}}^0 = \tilde{\Psi} = \widetilde{\mathbf{G}}_t\mathbf{F}_N^H\widehat{\mathbf{s}}$. Thus by using (15):

$$
\begin{aligned}
\widetilde{\mathbf{s}}^i &= \mathbf{F}_N^H\widehat{\mathbf{s}} - (\mathbf{I}_N - \widetilde{\mathbf{G}}_t)^i\left(\mathbf{F}_N^H\widehat{\mathbf{s}} - \widetilde{\mathbf{G}}_t\mathbf{F}_N^H\widehat{\mathbf{s}}\right) \\
&= \left(\mathbf{I}_N - (\mathbf{I}_N - \widetilde{\mathbf{G}}_t)^{i+1}\right)\mathbf{F}_N^H\widehat{\mathbf{s}} \\
&= \left[\sum_{j=1}^{i+1}\binom{i+1}{j}(-1)^{j-1}\widetilde{\mathbf{G}}_t^j\right]\mathbf{F}_N^H\widehat{\mathbf{s}}, \qquad (41)
\end{aligned}
$$

For arbitrary iteration of i, this is a closed form relation between the iterative block's output, $\widetilde{\mathbf{s}}^i$, and the LPF block's input, $\widehat{\mathbf{s}}$, in Fig. 2.

APPENDIX C
PROOF OF THE COMPENSATING ENERGY LEAKAGE IN PROPOSED ITERATIVE RECEIVER

We show how the energy leakage across subcarriers is compensated using our proposed iterative receiver. In other words, we will show that the error vector of $\widetilde{\mathbf{e}}^i = \widetilde{\mathbf{s}}^i - \widetilde{\mathbf{G}}_t^{\dagger}\widetilde{\mathbf{s}}^0 = \widetilde{\mathbf{s}}^i - \mathbf{F}_N^H\widehat{\mathbf{s}}$ (defined in Appendix B) decreases as the number of iteration i increases in our proposed iterative receiver. By considering the error vector, we can rewrite equation (17) as:

$$
\begin{cases}
\widetilde{\mathbf{e}}^i = (\mathbf{I}_N - \mathbf{G}_t)\,\widetilde{\mathbf{e}}^{i-1} & i > 0 \\
\widetilde{\mathbf{e}}^0 = \widetilde{\mathbf{s}}^0 - \mathbf{F}_N^H\widehat{\mathbf{s}} & i = 0,
\end{cases} \qquad (42)
$$

in which, we have $\widetilde{\mathbf{e}}^0 = \widetilde{\mathbf{s}}^0 - \mathbf{F}_N^H\hat{\mathbf{s}} = \boldsymbol{\Psi} - \mathbf{F}_N^H\hat{\mathbf{s}}$ for $i = 0$. From (42)

$$\begin{aligned}\widetilde{\mathbf{e}}^i &= (\mathbf{I}_N - \mathbf{G}_t)^i\widetilde{\mathbf{e}}^0 = (\mathbf{I}_N - \mathbf{G}_t)^i(\boldsymbol{\Psi} - \mathbf{F}_N^H\hat{\mathbf{s}}) \\ &= (\mathbf{I}_N - \mathbf{G}_t)^i(\mathbf{G}_t\mathbf{F}_N^H\hat{\mathbf{s}} - \mathbf{F}_N^H\hat{\mathbf{s}}) = -(\mathbf{I}_N - \mathbf{G}_t)^{i+1}\mathbf{F}_N^H\hat{\mathbf{s}}.\end{aligned} \tag{43}$$

Note that for simplicity we considered $\boldsymbol{\Psi}$ and $\mathbf{G}_t$ instead of $\widetilde{\boldsymbol{\Psi}}$ and $\widetilde{\mathbf{G}_t}$ in equation (42) (i.e., $\mathbf{E} = \mathbf{I}_N$).
Thus, from (28) and (43) we have:

$$\begin{aligned}\widetilde{\mathbf{e}}^i &= -\mathbf{V}\Lambda'^{i+1}\mathbf{V}^{-1}\mathbf{F}_N^H\hat{\mathbf{s}} \\ &= -\mathbf{V}\times\text{diag}\left((1-\lambda_1)^{i+1}, (1-\lambda_2)^{i+1}, \ldots, (1-\lambda_N)^{i+1}\right) \\ &\quad\times\mathbf{V}^{-1}\mathbf{F}_N^H\hat{\mathbf{s}}\end{aligned} \tag{44}$$

where eigenvectors of $\mathbf{G}_t$ are the matrix $\mathbf{V}$ columns and its eigenvalues is the matrix $\boldsymbol{\Lambda} = \text{diag}(\lambda_1, \lambda_2, \cdots, \lambda_N)$ and $\boldsymbol{\Lambda}' = \mathbf{I}_N - \boldsymbol{\Lambda}$. It is straightforward from (43) and (44) that the convergence of the algorithm (which compensates the energy leakage) is equivalent to the convergence of $\lim_{i\to\infty}(\mathbf{I}_N - \mathbf{G}_t)^{i+1}$
$= \mathbf{V}\times$
$\text{diag}\left((1-\lambda_1)^{i+1}, (1-\lambda_2)^{i+1}, \ldots, (1-\lambda_N)^{i+1}\right)$
$\times\mathbf{V}^{-1}$.
To assure convergence, we should have $|1-\lambda_m| \le 1$. Briefly, it is required that $\forall m : -1 \le 1-\lambda_m \le 1 \Rightarrow 0 \le \lambda_m \le 2 \Leftrightarrow$ *convergence* to assure compensating the energy leakage. Note that $\mathbf{G}_t = \text{diag}(g_{t1}, \ldots, g_{tN})$, $g_{tm} \in \{0, 1\}$ is a matrix with 1 and 0 entries on its diagonal that implies eigenvalues are $\lambda_m \in \{0, 1\}$. Therefore, the above convergence condition is satisfied for $\mathbf{G}_t$.

Assuming $\mathbf{G}_t$ with eigenvalues $\lambda_1, \lambda_2, \cdots, \lambda_N$ so that:

$$0 = \lambda_1 = \lambda_2 = \cdots = \lambda_c < \lambda_{c+1} \le \ldots \le \lambda_N, \tag{45}$$

where c is the number of zero eigenvalues ($0 \le c \le N$). If $\mathbf{G}_t$ is an invertible matrix, it has no zero eigenvalues ($c = 0$ in (45)) and thus for all m, $|1-\lambda_m| \le 1$. This means $\widetilde{\mathbf{e}}^i \to 0$ as $i \to \infty$ and hence from the definition of the error vector of $\widetilde{\mathbf{e}}^i = \widetilde{\mathbf{s}}^i - \mathbf{F}_N^H\hat{\mathbf{s}}$ we have $\lim_{k\to\infty}\widetilde{\mathbf{s}}^i = \mathbf{F}_N^H.\hat{\mathbf{s}}$. From this equation, a perfect signal reconstruction and hence complete compensation of the energy leakage that may occur due to the $\mathbf{G}_f$ is shown. Now let us assume that $\mathbf{G}_t$ is not invertible and has c zero eigenvalues. As a consequence, $\mathbf{I}_N - \mathbf{G}_t$ has c eigenvalues equal to 1 and the rest have absolute values less than 1.

$$\begin{aligned}&(\mathbf{I}_N - \mathbf{G}_t)^{i+1} = \mathbf{V} \\ &\quad\times\text{diag}\left(\underbrace{1, 1, \ldots, 1}_{c\text{times}}, (1-\lambda_{c+1})^{i+1}, \ldots, (1-\lambda_N)^{i+1}\right) \\ &\quad\times\mathbf{V}^{-1} \\ &\Rightarrow (\mathbf{I}_N - \mathbf{G}_t)^{\infty} = \lim_{i\to\infty}(\mathbf{I}_N - \mathbf{G}_t)^{i+1} \\ &= \mathbf{V}\text{diag}\left(\underbrace{1, 1, \ldots, 1}_{c\text{times}}, \underbrace{0, \ldots, 0}_{N-c\text{times}}\right)\mathbf{V}^{-1} \\ &\Rightarrow \tilde{\mathbf{s}}^{\infty} = \lim_{i\to\infty}\tilde{\mathbf{s}}^i = \lim_{i\to\infty}(\mathbf{I}_N - (\mathbf{I}_N - \mathbf{G}_t)^{i+1})\mathbf{F}_N^H\hat{\mathbf{s}} \\ &= (\mathbf{I}_N - (\mathbf{I}_N - \mathbf{G}_t)^{\infty})\mathbf{F}_N^H\hat{\mathbf{s}} \\ &= \mathbf{V}\text{diag}\left(\underbrace{0, 0, \ldots, 0}_{c\text{times}}, \underbrace{1, \ldots, 1}_{N-c\text{times}}\right)\mathbf{V}^{-1}\mathbf{F}_N^H\hat{\mathbf{s}}\end{aligned} \tag{46}$$

Now we show that the same result is also obtained by pseudo-inverse of $\mathbf{G}_t$.

$$\begin{aligned}&\mathbf{G}_t = \mathbf{V}\text{diag}\left(\underbrace{0, 0, \ldots, 0}_{c\text{ times}}, \lambda_{c+1}, \ldots, \lambda_N\right)\mathbf{V}^{-1} \\ &\Rightarrow \mathbf{G}_t^{\dagger} = \mathbf{V}\text{diag}\left(\underbrace{0, 0, \ldots, 0}_{c\text{ times}}, \lambda_{c+1}^{-1}, \ldots, \lambda_N^{-1}\right)\mathbf{V}^{-1} \\ &\Rightarrow \mathbf{G}_t^{\dagger}\mathbf{G}_t = \mathbf{V}\text{diag}\left(\underbrace{0, 0, \ldots, 0}_{c\text{ times}}, 1, \ldots, 1\right)\mathbf{V}^{-1} \\ &\Rightarrow \mathbf{F}_N^H\hat{\mathbf{s}} = \mathbf{G}_t^{\dagger}\mathbf{G}_t\mathbf{F}_N^H\hat{\mathbf{s}} \\ &= \mathbf{V}\text{diag}\left(\underbrace{0, 0, \ldots, 0}_{c\text{ times}}, 1, \ldots, 1\right)\mathbf{V}^{-1}\mathbf{F}_N^H\hat{\mathbf{s}}\end{aligned} \tag{47}$$

Comparing (46) and (47), we get $\tilde{\mathbf{s}}^{\infty} = \mathbf{F}_N^H\hat{\mathbf{s}} \to \tilde{\mathbf{e}}^{\infty} = 0$. Therefore, it is proved that when the matrix $\mathbf{G}_t$ is not invertible, the iterative receiver converges to the solution. In other words, the energy leakage across subcarriers is compensated.

APPENDIX D
PROOF OF THE LEMMA 4

By expanding the simplified system model in (29), we have:

$$\begin{aligned}&\mathbf{V}(\mathbf{I}_N - \Lambda'^{i+1})\mathbf{V}^{-1} \\ &= \begin{pmatrix}\mathbf{a}_1 \\ \vdots \\ \mathbf{a}_N\end{pmatrix}\begin{pmatrix}1-\lambda_1'^{i+1} & & 0 \\ & \ddots & \\ 0 & & 1-\lambda_N'^{i+1}\end{pmatrix}(\mathbf{b}_1, \cdots, \mathbf{b}_N) \\ &= \begin{pmatrix}\sum_{t=1}^{N} a_{1t}b_{1t}(1-\lambda_t'^{i+1}) & \ldots & \sum_{t=1}^{N} a_{1t}b_{Nt}(1-\lambda_t'^{i+1}) \\ \vdots & & \vdots \\ \sum_{t=1}^{N} a_{Nt}b_{1t}(1-\lambda_t'^{i+1}) & \cdots & \sum_{t=1}^{N} a_{Nt}b_{Nt}(1-\lambda_t'^{i+1})\end{pmatrix},\end{aligned} \tag{48}$$

where, $\mathbf{a}_j = [a_{j1}, \ldots, a_{jN}]$, $\mathbf{b}_j = [b_{j1}, \ldots, b_{jN}]^T$ for $j = 1, 2, \ldots, N$ are rows and columns of matrix $\mathbf{V}$ and $\mathbf{V}^{-1}$, respectively. It is obvious that the Hadamard matrix product of the vectors $\mathbf{a}_m$ and $\mathbf{b}_n^T$ can be obtained from

$\mathbf{a}_m \circ \mathbf{b}_n^T = \begin{cases} 1 & m = n \\ 0 & m \neq n \end{cases}$. Hence:

$$\mathbf{p} = \begin{pmatrix} u_1 \sum_{t=1}^{N} a_{1t} b_{1t} (1-\lambda_t^{'i+1}) + \cdots + u_N \sum_{t=1}^{N} a_{1t} b_{Nt} (1-\lambda_t^{'i+1}) \\ \vdots \\ u_1 \sum_{t=1}^{N} a_{Nt} b_{1t} (1-\lambda_t^{'i+1}) + \cdots + u_N \sum_{t=1}^{N} a_{Nt} b_{Nt} (1-\lambda_t^{'i+1}) \end{pmatrix}$$
$$= \begin{pmatrix} \sum_{j=1}^{N} \left(u_j \sum_{t=1}^{N} a_{1t} b_{jt} (1-\lambda_t^{'i+1}) \right) \\ \vdots \\ \sum_{j=1}^{N} \left(u_j \sum_{t=1}^{N} a_{Nt} b_{jt} (1-\lambda_t^{'i+1}) \right) \end{pmatrix} \quad (49)$$

Thus after averaging on the Hadamard matrix product of the vectors $\bar{\mathbf{p}}$ and $\mathbf{p}$ we obtain

$$E[\bar{\mathbf{p}} \circ \mathbf{p}] = \begin{pmatrix} \sum_{j=1}^{N} \sigma_{u_j}^2 \left\| \sum_{t=1}^{N} a_{1t} b_{jt} (1-\lambda_t^{'i+1}) \right\|_2 \\ \vdots \\ \sum_{j=1}^{N} \sigma_{u_j}^2 \left\| \sum_{t=1}^{N} a_{Nt} b_{jt} (1-\lambda_t^{'i+1}) \right\|_2 \end{pmatrix}$$
$$= \left\| \mathbf{V}(\mathbf{I}_N - \Lambda^{'i+1}) \mathbf{V^{-1}} \right\|_2 \mathrm{diag}(\sigma_{u_1}^2, \sigma_{u_2}^2, \ldots, \sigma_{u_N}^2) \mathbf{I}_{N \times 1}. \quad (50)$$

Hence, the jth subchannel noise variance σ_{pj}^2, jth entry of vector $E[\bar{\mathbf{p}} \circ \mathbf{p}]$, is given in equation (50).

REFERENCES

[1] G. Femenias and F. Riera-Palou, "Scheduling and resource allocation in downlink multiuser MIMO-OFDMA systems," *IEEE Transactions on Communications*, vol. 64, no. 5, pp. 2019–2034, 2016.
[2] G. Kaddoum, "Design and performance analysis of a multiuser OFDM based differential chaos shift keying communication system," *IEEE Transactions on Communications*, vol. 64, no. 1, pp. 249–260, 2016.
[3] P. Kryszkiewicz and H. Bogucka, "In-band-interference robust synchronization algorithm for an NC-OFDM system," *IEEE Transactions on Communications*, vol. 64, no. 5, pp. 2143–2154, 2016.
[4] Y. S. Jeon, H. M. Kim, Y. S. Cho, and G. H. Im, "Time-domain differential feedback for massive MISO-OFDM systems in correlated channels," *IEEE Transactions on Communications*, vol. 64, no. 2, pp. 630–642, 2016.
[5] A. Hajisami and D. Pompili, "Cloud-CFFR: Coordinated fractional frequency reuse in cloud radio access network (C-RAN)," in *2015 IEEE 12th International Conference on Mobile Ad Hoc and Sensor Systems*, 2015, pp. 46–54.
[6] M. Korki, J. Zhang, C. Zhang, and H. Zayyani, "Block-sparse impulsive noise reduction in OFDM systems a novel iterative bayesian approach," *IEEE Transactions on Communications*, vol. 64, no. 1, pp. 271–284, 2016.
[7] Q. Li, J. Zhang, and U. Epple, "Design and exit chart analysis of a doubly iterative receiver for mitigating impulsive interference in OFDM systems," *IEEE Transactions on Communications*, vol. 64, no. 4, pp. 1726–1738, 2016.
[8] A. A. D'Amico, L. Marchetti, M. Morelli, and M. Moretti, "Frequency estimation in OFDM direct-conversion receivers using a repeated preamble," *IEEE Transactions on Communications*, vol. 64, no. 3, pp. 1246–1258, 2016.
[9] J. Francis, N. B. Mehta, and S. N. Ananya, "Best-M feedback in OFDM: Base-station-side estimation and system implications," *IEEE Transactions on Wireless Communications*, vol. 15, no. 5, pp. 3616–3627, 2016.
[10] L. Chang, G. Y. Li, J. Li, and R. Li, "Blind parameter estimation of GFDM signals over frequency-selective fading channels," *IEEE Transactions on Communications*, vol. 64, no. 3, pp. 1120–1131, 2016.
[11] E. Panayirci, H. Senol, M. Uysal, and H. V. Poor, "Sparse channel estimation and equalization for OFDM-based underwater cooperative systems with amplify-and-forward relaying," *IEEE Transactions on Signal Processing*, vol. 64, no. 1, pp. 214–228, 2016.
[12] J. Lacruz, J. RamÃrez, and J. Paredes, "Robust sparse channel estimation for OFDM system using an iterative algorithm based on complex median," in *2014 IEEE International Conference on Acoustics, Speech and Signal Processing (ICASSP)*, 2014, pp. 6429–6433.
[13] W. Bajwa, J. Haupt, A. Sayeed, and R. Nowak, "Compressed channel sensing: A new approach to estimating sparse multipath channels," *Proceedings of the IEEE*, vol. 98, no. 6, pp. 1058–1076, Jun. 2010.
[14] M. M. Hyder and K. Mahata, "A sparse recovery method for initial uplink synchronization in OFDMA systems," *IEEE Transactions on Communications*, vol. 64, no. 1, pp. 377–386, 2016.
[15] Y. Zhang, R. Venkatesan, O. A. Dobre, and C. Li, "Novel compressed sensing-based channel estimation algorithm and near-optimal pilot placement scheme," *IEEE Transactions on Wireless Communications*, vol. 15, no. 4, pp. 2590–2603, 2016.
[16] D. Wang, Y. Cao, and L. Zheng, "Efficient two-stage discrete bit-loading algorithms for OFDM systems," *IEEE Trans. Veh. Technol.*, vol. 59, no. 7, pp. 3407 – 3416, Sept. 2010.
[17] E. H. Choi, W. Choi, J. G. Andrews, and B. F. Womack, "Power loading using order mapping in OFDM systems with limited feedback," *IEEE Signal Process. Lett.*, vol. 15, no. 5, pp. 545 – 548, Sept. 2008.
[18] T. N. Vo, K. Amis, T. Chonavel, and P. Siohan, "A low-complexity bit-loading algorithm for OFDM systems under spectral mask constraint," *IEEE Communications Letters*, vol. 20, no. 6, pp. 1076–1079, 2016.
[19] L. Zhu, Y. Pei, N. Ge, J. Lu, and Z. Xu, "A signal subspace detection technique for single carrier block transmission with unique words," *IEEE Commun. Lett.*, vol. 15, no. 2, pp. 151–153, Feb. 2011.
[20] L. Dai, J. Wang, Z. Wang, P. Tsiaflakis, and M. Moonen, "Spectrally efficient multicarrier transmission with message-driven subcarrier selection," *IEEE Trans. Signal Process.*, vol. 61, no. 23, pp. 6047–6059, Dec. 2013.
[21] X. Zhang, H. Guo, and Y. Zhao, "A Low-Complexity adaptive Co-Channel interference removal scheme for COFDM systems," *IEEE Trans. Consumer Electronics*, vol. 56, no. 2, pp. 353 – 358, May 2010.
[22] X. Liu and H.-C. Wu, "Novel asterisk 16QAM constellation for COFDM," *IEEE Commun. Lett.*, vol. 14, no. 7, pp. 596 – 598, Jul. 2010.
[23] S. Wang, S. Zhu, and G. Zhang, "A walsh-hadamard coded spectral efficient full frequency diversity OFDM system," *IEEE Transactions on Communications*, vol. 58, no. 1, pp. 28–34, 2010.
[24] J. L. Yu and D. Y. Hong, "A novel subspace channel estimation with fast convergence for ZP-OFDM systems," *IEEE Transactions on Wireless Communications*, vol. 10, no. 10, pp. 3168–3173, 2011.
[25] D. Chen, X. G. Xia, T. Jiang, and X. Gao, "Properties and power spectral densities of CP based OQAM-OFDM systems," *IEEE Transactions on Signal Processing*, vol. 63, no. 14, pp. 3561–3575, 2015.
[26] L. Dai, Z. Wang, and Z. Yang, "Time-frequency training OFDM with high spectral efficiency and reliable performance in high speed environments," *IEEE J. Sel. Areas Commun.*, vol. 30, no. 4, pp. 695–707, May 2012.
[27] G. Dziwoki and J. Izydorczyk, "Iterative identification of sparse mobile channels for TDS-OFDM systems," *IEEE Transactions on Broadcasting*, vol. 62, no. 2, pp. 384–397, 2016.
[28] B. Muquet, Z. Wang, G. B. Giannakis, M. de Courville, and P. Duhamel, "Cyclic prefixing or zero padding for wireless multicarrier transmissions?" *IEEE Trans. Commun.*, vol. 50, no. 12, pp. 2136–2148, Dec. 2002.
[29] M. Ma, X. Huang, B. Jiao, and Y. J. Guo, "Optimal orthogonal precoding for power leakage suppression in DFT-based systems," *IEEE Trans. Commun.*, vol. 59, no. 3, pp. 844–853, Mar. 2011.
[30] A. S. Bedi, J. Akhtar, K. Rajawat, and A. K. Jagannatham, "BER-optimized precoders for OFDM systems with insufficient cyclic prefix," *IEEE Communications Letters*, vol. 20, no. 2, pp. 280–283, 2016.

[31] X. Huang, J. A. Zhang, and Y. J. Guo, "Out-of-band emission reduction and a unified framework for precoded OFDM," *IEEE Communications Magazine*, vol. 53, no. 6, pp. 151–159, 2015.
[32] E. Balevi and A. O. Yilmaz, "Analysis of frequency domain oversampled MMSE SC-FDE," *IEEE Communications Letters*, vol. 20, no. 2, pp. 232–235, 2016.
[33] T. W. Wu and C. D. Chung, "Spectrally precoded DFT-based OFDM and OFDMA with oversampling," *IEEE Transactions on Vehicular Technology*, vol. 63, no. 6, pp. 2769–2783, 2014.
[34] A. Rahmati and P. Azmi, "Iterative reconstruction of oversampled OFDM signals over deep fading channels," in *Circuits and Systems for Communications, 2008. ECCSC 2008. 4th European Conference on*, 2008, pp. 289–294.
[35] ——, "Performance analysis of nonuniform sampling based iterative equalizer for OFDM signals," in *Telecommunications (IST), 2010 5th International Symposium on*, 2010, pp. 685–690.
[36] ——, "POE analysis of time domain iterative detection algorithm for oversampled OFDM systems over fading channels," in *Computer Modeling and Simulation (EMS), 2010 Fourth UKSim European Symposium on*, 2010, pp. 514–519.
[37] A. Rahmati, K. Raahemifar, A. Anpalagan, T. A. Tsiftsis, P. Azmi, and N. I. Miridakis, "Superposition modulation-based cooperation for oversampled OFDM signals," *IEEE Transactions on Communication*, vol. 65, no. 11, pp. 4791–4802, 2017.
[38] L. H. Grokop and D. N. C. Tse, "Diversity multiplexing tradeoff in ISI channels," *IEEE Transactions on Information Theory*, vol. 55, no. 1, pp. 109–135, 2009.
[39] R. Xu, J. Zhang, M. Chen, B. Wu, and H. Wang, "Pairwise subcarriers weighting for suppressing out-of-band radiation of OFDM," *International Journal of Communication Systems*, vol. 25, no. 1, pp. 16 – 29, Jan. 2012.
[40] H. Schulze and C. Luders, *Theory and Applications of OFDM and CDMA*. Wiley, 2005.
[41] L. Yang and J. Armstrong, "Oversampling to reduce the effect of timing jitter on high speed OFDM systems," *IEEE Communications Letters*, vol. 14, no. 3, pp. 196–198, 2010.
[42] B. Chen and H. Wang, "Blind estimation of OFDM carrier frequency offset via oversampling," *IEEE Transactions on Signal Processing*, vol. 52, no. 7, pp. 2047–2057, 2004.
[43] Y. Yan and M. Ma, "Novel frequency-domain oversampling receiver for CP MC-CDMA systems," *IEEE Communications Letters*, vol. 19, no. 4, pp. 661–664, 2015.
[44] B. Peng, P. S. Rossi, H. Dong, and K. Kansanen, "Time-domain oversampled OFDM communication in doubly-selective underwater acoustic channels," *IEEE Communications Letters*, vol. 19, no. 6, pp. 1081–1084, 2015.
[45] S. Gazor and R. AliHemmati, "Tone reservation for OFDM systems by maximizing signal-to-distortion ratio," *IEEE Transactions on Wireless Communications*, vol. 11, no. 2, pp. 762–770, 2012.
[46] S. Ono and I. Yamada, "Signal recovery with certain involved convex data-fidelity constraints," *IEEE Transactions on Signal Processing*, vol. 63, no. 22, pp. 6149–6163, 2015.
[47] J. Wang, S. Kwon, P. Li, and B. Shim, "Recovery of sparse signals via generalized orthogonal matching pursuit: A new analysis," *IEEE Transactions on Signal Processing*, vol. 64, no. 4, pp. 1076–1089, 2016.
[48] S. C. Pei and S. G. Huang, "Fast discrete linear canonical transform based on CM-CC-CM decomposition and FFT," *IEEE Transactions on Signal Processing*, vol. 64, no. 4, pp. 855–866, 2016.
[49] M. A. Davenport and J. Romberg, "An overview of low-rank matrix recovery from incomplete observations," *IEEE Journal of Selected Topics in Signal Processing*, vol. 10, no. 4, pp. 608–622, 2016.
[50] S. Xu, R. C. de Lamare, and H. V. Poor, "Distributed compressed estimation based on compressive sensing," *IEEE Signal Processing Letters*, vol. 22, no. 9, pp. 1311–1315, 2015.
[51] F. Marvasti, *Theory and Practice of Nonuniform Sampling*. Kluwer Academic/Plenum Publishers, New-York, 2001.
[52] F. Marvasti, M. Hasan, M. Echhart, and S. Talebi, "Efficient algorithms for burst error recovery using FFT and other transform kernels," *IEEE Transactions on Signal Processing*, vol. 47, no. 4, pp. 1065–1075, 1999.
[53] J. G. Proakis, *Digital Communications*. New York: McGraw-Hill, 1995.
[54] S. F. A. Shah and A. H. Tewfik, "Design and analysis of post-coded ofdm systems," *IEEE Trans. Wireless Commun.*, vol. 7, no. 12, pp. 4907–4918, Dec. 2008.
[55] G. H. Golub and C. F. V. Loan, *Matrix Computations*. Baltimore, MD: Johns Hopkins Univ. Press, 1996.
[56] K. B. Petersen and M. S. Pedersen, *The Matrix Cookbook*. Version: Nov. 14, 2008.
[57] S. Verdu and T. Weissman, "The information lost in erasures," *IEEE Transactions on Information Theory*, vol. 54, no. 11, pp. 5030–5058, 2008.

ALIREZA RAHMATI was born in Tehran, Iran, in 1981. He received the B.Sc. degree in electrical engineering from the Sharif University of Technology, Tehran, in 2004, and the M.Sc. and Ph.D. degrees in telecommunication systems engineering from Tarbiat Modares University, Tehran, in 2007 and 2012, respectively. He is currently a Post-Doctoral Fellow at the Department of Electrical and Computer Engineering, Ryerson University, Toronto, ON, Canada. From 2007 to 2015, he was with the Advanced Electronic and Communication Research Center, Tehran. Also, he has been with GT Global Service Inc., Markham, ON, Canada, involved in the studies for the M2M communications and LTE network. His main research interests are statistical signal processing, navigation and positioning, 5G relay networks, and full-duplex radio. He serves as a reviewer and TPC member for several prestigious international journals and conferences.

KAAMRAN RAAHEMIFAR (S'91–M'99–SM'02) received the B.Sc. degree in electrical engineering from the Sharif University of Technology, Tehran, Iran, in 1988, the M.A.Sc. degree from Electrical and Computer Engineering Department, Waterloo University, Waterloo, ON, Canada, in 1993, and the Ph.D. degree from Windsor University, Windsor, ON, Canada. He joined Ryerson University in 1999 and was tenured in 2001. Since 2011, he has been a Professor with the Department of Electrical and Computer Engineering, Ryerson University. His research interests include VLSI circuit simulation, design, and testing, signal processing and hardware implementation of biomedical signals. He was a recipient of the ELCE-GSA Professor of the Year Award (Elected by Graduate Student's Body, 2010), the Faculty of Engineering, Architecture, and Science Best Teaching Award (April 2011), the Department of Electrical and Computer Engineering Best Teaching Award (December 2011), and the Research Award (December 2014). He has been awarded more than $6M external research fund during his time at Ryerson.

THEODOROS A. TSIFTSIS (S'02–M'04–SM'10) was born in Lamia, Greece, in 1970. He received the B.Sc. degree in physics from the Aristotle University of Thessaloniki, Greece, in 1993, the M.Sc. degree in digital systems engineering from Heriot-Watt University, Edinburgh, U.K., in 1995, the M.Sc. degree in decision sciences from the Athens University of Economics and Business, in 2000, and the Ph.D. degree in electrical engineering from the University of Patras, Greece, in 2006. He joined the Technological Educational Institute of Central Greece in 2010. He is currently an Associate Professor in communication technologies with the School of Engineering, Nazarbayev University, Astana, Kazakhstan. He has authored or co-authored over 120 technical papers in scientific journals and international conferences. His research interests include the broad areas of cooperative communications, cognitive radio, communication theory, wireless powered communication systems, and optical wireless communication systems.

Dr. Tsiftsis acts as a reviewer for several international journals and conferences. He has served as Senior or Associate Editor in the Editorial Boards for the IEEE TRANSACTIONS ON VEHICULAR TECHNOLOGY and the IEEE COMMUNICATIONS LETTERS. He is currently an Area Editor for Wireless Communications II of the IEEE TRANSACTIONS ON COMMUNICATIONS and an Associate Editor of the IEEE TRANSACTIONS ON MOBILE COMPUTING.

ALAGAN ANPALAGAN received the B.A.Sc., M.A.Sc., and Ph.D. degrees in electrical engineering from the University of Toronto, Canada. He joined the Department of Electrical and Computer Engineering, Ryerson University, in 2001, and was promoted to Full Professor in 2010. He served the Department as the Graduate Program Director (2004–2009) and the Interim Electrical Engineering Program Director (2009-2010). During his sabbatical (2010-2011), he was a Visiting Professor at Asian Institute of Technology and a Visiting Researcher at Kyoto University.

Dr. Anpalagan directs a research group working on radio resource management and radio access & networking areas within the WINCORE Laboratory. His current research interests include cognitive radio resource allocation and management, wireless cross layer design and optimization, collaborative communication, green communications technologies, machine-to-machine communication, and small cell networks. He is a co-author/editor of the books *Small Cell Networks* (Cambridge Press, 2014), the Handbook of *Green Information and Communication Systems* (Academic Press, 2012), and *Routing in Opportunistic Networks* (Springer-Verlag, 2013). He has published more than 200 technical papers in his research areas.

Dr. Anpalagan serves as an Associate Editor for the IEEE COMMUNICATIONS SURVEYS & TUTORIALS (2012–), the IEEE COMMUNICATIONS LETTERS (2010–2013), and *Springer Wireless Personal Communications* (2009–), and past Editor for the *EURASIP Journal of Wireless Communications and Networking* (2004–2009). He also served as a Guest Editor for special issues in *ACM/Springer MONET Green Cognitive and Cooperative Communication and Networking* (2012), *EURASIP Radio Resource Management in 3G+ Systems* (2006), and *EURASIP Fairness in Radio Resource Management for Wireless Networks* (2008).

Dr. Anpalagan held various positions within the IEEE Canada, including the Chair, IEEE Central Canada, the Chair (2013-), IEEE Canada Professional Activities Committee (2009-2011), th eIEEE Toronto Section Chair (2006-07), and the ComSoc Toronto Chapter Chair (2004–2005). He was a recipient of the Dean's Teaching Award (2011), the Faculty Scholastic, Research and Creativity Award (2010), and the Faculty Service Award (2010) at Ryerson University. He also completed a course on Project Management for Scientist and Engineers at the University of Oxford CPD Center. He is a registered Professional Engineer in the province of Ontario, Canada.

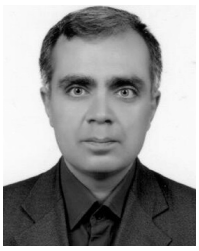

PAEIZ AZMI (M'09–SM'10) was born in Tehran, Iran, in 1974. He received the B.Sc., M.Sc., and Ph.D. degrees in electrical engineering from the Sharif University of Technology, Tehran, in 1996, 1998, and 2002, respectively. Since 2002, he has been with the Electrical and Computer Engineering Department, Tarbiat Modares University, Tehran, where he became an Associate Professor in 2006 and he is currently a Full Professor. From 1999 to 2001, he was with the Advanced Communication Science Research Laboratory, Iran Telecommunication Research Center (ITRC), Tehran. From 2002 to 2005, he was with the Signal Processing Research Group, ITRC. His current research interests include modulation and coding techniques, digital signal processing, wireless communications, and estimation and detection theories.